**REPUBLIC OF TÜRKİYE**
**YILDIZ TECHNICAL UNIVERSITY**
**GRADUATE SCHOOL OF SCIENCE AND ENGINEERING**

# HUMAN DETECTION THROUGH WALLS USING FMCW RADAR SENSOR

**Zainab Elfatih Mohamed MALIK**

MASTER OF SCIENCE THESIS
Department of Computer Engineering
Program of Computer Engineering

Supervisor
Prof. Dr. Mine Elif KARSLIGİL

Co-supervisor
Asst. Prof. Ziya Cihan TAYŞİ

July, 2024

**REPUBLIC OF TÜRKİYE**
**YILDIZ TECHNICAL UNIVERSITY**
**GRADUATE SCHOOL OF SCIENCE AND ENGINEERING**

# HUMAN DETECTION THROUGH WALLS USING FMCW RADAR SENSOR

A thesis submitted by Zainab Elfatih Mohamed MALIK in partial fulfillment of the requirements for the degree of **MASTER OF SCIENCE** is approved by the committee on 25.07.2024 in Department of Computer Engineering, Program of Computer Engineering.

Prof. Dr. Mine Elif KARSLIGİL
Yildiz Technical University
Supervisor

Asst. Prof. Ziya Cihan TAYŞİ
Yildiz Technical University
Co-supervisor

**Approved By the Examining Committee**

Prof. Dr. Mine Elif KARSLIGİL, Supervisor
Yildiz Technical University _____

Assoc. Prof. FEZA BUZLUCA, Member
Istanbul Technical University _____

Assoc. Prof. MEHMET AMAÇ GÜVENSAN, Member
Yildiz Technical University _____

I hereby declare that I have obtained the required legal permissions during data collection and exploitation procedures, that I have made the in-text citations and cited the references properly, that I haven't falsified and/or fabricated research data and results of the study and that I have abided by the principles of the scientific research and ethics during my Thesis Study under the title of HUMAN DETECTION THROUGH WALLS USING FMCW RADAR SENSOR supervised by my supervisor, Prof. Dr. Mine Elif KARSLIGİL. and my co-supervisor, Asst. Prof. Ziya Cihan TAYŞİ. In the case of a discovery of false statement, I am to acknowledge any legal consequence.

Zainab Elfatih Mohamed MALIK

Signature

*Dedicated to my family*
*and my country, Sudan*

# ACKNOWLEDGEMENTS

I am deeply grateful for the completion of this thesis. I would like to express my heartfelt thanks to my understanding supervisors, Prof. Dr. Mine Elif KARSLIGİL and Asst. Prof. Ziya Cihan TAYŞİ, for their invaluable guidance and encouragement throughout this journey. Their support was instrumental in helping me achieve this milestone.

I extend my sincere thanks to Prof. Dr. Ali Gökhan Yavuz for his help in guiding me to choose a suitable sensor and data collection process, and to Dr. Aisha Sir-Alkhatim for her continual support and guidance.

I extend my gratitude to my entire family, who, despite being in a war-torn area, have continued to motivate and believe in me. I am profoundly grateful to my father, Elfatih Malik, who has been my role model in research and exemplifies hard work regardless of circumstances. I also thank my mother Hanan for always believing in me, and my siblings Duha, Sara and Mohammed for their constant support.

Special thanks to Esenler Ensar Vakfi dormitory for providing me with the opportunity to collect data at the dormitory and to all my friends their especially, Souhayla. Your support and cooperation were essential in conducting this research effectively.

The encouragement and belief of those around me provided the strength and motivation needed to persevere and reach this accomplishment. Their unwavering support has been a source of inspiration and resilience, and I am forever thankful for their presence in my life.

Zainab Elfatih Mohamed MALIK

# TABLE OF CONTENTS

**LIST OF SYMBOLS** vii

**LIST OF ABBREVIATIONS** viii

**LIST OF FIGURES** x

**LIST OF TABLES** xii

**ABSTRACT** xiii

**ÖZET** xiv

**1 INTRODUCTION** 1

1.1 Background . . . . . 1

1.2 Research Motivation . . . . . 1

1.3 Problem Statement . . . . . 2

**2 LITERATURE REVIEW** 4

2.1 Technologies for Human Detection Through Wall . . . . . 4

2.2 Importance and Applications of Through-Wall Human Detection . . . . . 6

2.3 Radar Sensor Technology in Through Wall Applications . . . . . 7

2.4 Machine Learning for Human Detection Through Wall . . . . . 12

2.5 Commercially Available Industrial Sensors for Human Detection . . . . . 13

**3 METHODOLOGY** 14

3.1 Preprocessing . . . . . 15

3.1.1 Window Slicing . . . . . 15

3.1.2 Feature Scaling . . . . . 15

3.2 Feature Engineering . . . . . 16

3.2.1 Feature Extraction . . . . . 16

3.2.2 Feature Selection . . . . . 18

3.3 Human Detection Models . . . . . 19

**4 DATA COLLECTION** 23

4.1 FMCW Working Principle . . . 23
4.2 Sensor Overview . . . 23
4.3 Data Collection Setups . . . 28
4.3.1 Investigate FMCW Sensor for Action Recognition When No Barriers Exist . . . 30
4.3.2 Behind Wall Dataset . . . 31

**5 RESULTS AND DISCUSSION** **38**
5.1 Through Wall Human Detection . . . 38
5.1.1 Data Scaling . . . 38
5.1.2 Feature Extraction and Selection . . . 38
5.1.3 Human Detection Models . . . 40
5.1.4 The Effect of Feature Selection on System Performance . . . 42
5.2 Through Wall Action Recognition . . . 44
5.2.1 Initial Three Classes Classification . . . 45
5.2.2 Merging Classes into Static and Movement . . . 47
5.3 Out-of-Sample Testing . . . 48

**6 CONCLUSION** **54**

**REFERENCES** **56**

**A SORTED FEATURES FOR ACTION RECOGNITION** **62**

**PUBLICATIONS FROM THE THESIS** **63**

# LIST OF SYMBOLS

| | |
|---|---|
| $C_i$ | Combined importance score for the $i$-th feature |
| Pcum | Cumulative power |
| E | Energy of the signal |
| fi | Frequency of the i-th component |
| $\Delta x$ | First derivative of the signal |
| H | H-function (Entropy) |
| I | Indicator function |
| xi | i-th sample |
| $\text{MI}_i$ | Importance score for the $i$-th feature from Mutual Information |
| $\text{RF}_i$ | Importance score for the $i$-th feature from Random Forest |
| $\text{RFE}_i$ | Importance score for the $i$-th feature from Recursive Feature Elimination |
| max(x) | Maximum value of the signal |
| $\mu$ | Mean value |
| med(x) | Median of the signal |
| min(x) | Minimum value of the signal |
| N | Number of samples in the signal or frequency components |
| P | Power of the signal |
| Pi | Power at frequency component i |
| pi | Probability of the i-th value |
| RMS | Root Mean Square |
| x | Signal |
| $\sigma$ | Standard deviation |
| Var(x) | Variance of the signal |

# LIST OF ABBREVIATIONS

| | |
|---|---|
| ADC | Analog-to-Digital Conversion |
| AUC-ROC | Area Under the Curve - Receiver Operating Characteristic |
| BR | Breathing Rate |
| CCTV | Closed-circuit Television |
| CNN | Convolutional Neural Network |
| CW | Continuous Wave |
| DAFE | Data Augmentation Feature Extraction |
| DT | Decision Tree |
| FFT | Fast Fourier Transform |
| FMCW | Frequency Modulated Continuous Wave |
| HR | Heart Rate |
| KNN | K-Nearest Neighbors |
| LR | Logistic Regression |
| LSTM | Long Short-Term Memory |
| MCU | Microcontroller Unit |
| mmWave | Millimeter-wave |
| MODWT | Maximal Overlap Discrete Wavelet Transform |
| NB | Naive Bayes |
| NLOS | Non-Line-of-Sight |
| MI | Mutual Information(Information gain) |
| PIR | Passive Infrared |
| PSD | Power Spectrum Density |
| RFE | Recursive Feature Elimination |

| | |
|---|---|
| RF | Random Forest |
| SFCW | Stepped Frequency Continuous Wave |
| SVD | Singular Value Decomposition |
| SVM | Support Vector Machine |
| TWP-CNN | Through-Wall Penetration Convolutional Neural Network |
| UWB | Ultra-Wideband |

# LIST OF FIGURES


**Figure 2.1** Frequency Vs. Wall Thickness Distribution in Literature . . . . . 11
**Figure 3.1** System Overview. . . . . 14
**Figure 3.2** Correlation Matrix. . . . . 20
**Figure 3.3** Scatter Matrix . . . . . 20
**Figure 4.1** FMCW Signal Pattern . . . . . 24
**Figure 4.2** HB100 Testing Experiments . . . . . 24
**Figure 4.3** RCWL 0516 Testing Experiments . . . . . 25
**Figure 4.4** RCWL 0516 Testing Environment . . . . . 25
**Figure 4.5** Seeed Studio Human Detection Module output . . . . . 25
**Figure 4.6** mmWave FMCW Human Presence Module . . . . . 27
**Figure 4.7** Operating Principle . . . . . 27
**Figure 4.8** Default Installation Setup . . . . . 28
**Figure 4.9** Arduino/Sensor Interface. . . . . 29
**Figure 4.10** Data Collection Scenarios a) Static, b) Slow Motion, c) Fast Motion. . . . 30
**Figure 4.11** Data Collection Environment a) Sensor Installation Behind Brick Wall, b) Brick Wall 17 cm Thickness, c) Wooden Door 4 cm Thickness. . . . . 30
**Figure 4.12** Processed Output from Sensor When No Barriers Exist . . . . . 31
**Figure 4.13** Different Motion When No Barriers - Volunteer 1 . . . . . 32
**Figure 4.14** Different Motion When No Barriers - Volunteer 2 . . . . . 32
**Figure 4.15** Detecting Human Presence and Activity Through Different Materials; No wall, Wooden wall and Brick wall Respectively. . . . . 33
**Figure 4.16** Sensor Readings for Different Wall Types with No Human Presence. . . . . 34
**Figure 4.17** Sensor Readings for Different Wall Types with Static Human. . . . . 34
**Figure 4.18** Sensor Readings for Different Distances Behind 4cm Wooden Wall . . . . 35
**Figure 4.19** Sensor Readings for Different Distances Behind 17 cm Brick Wall . . . . . 35
**Figure 4.20** Sensor Readings for Different Types of Movements Behind 4 cm Wooden Wall. . . . . 36
**Figure 4.21** Sensor Readings for Different Movements Behind 17 cm Brick Wall. . . . 36
**Figure 4.22** Sensor Readings for Different Movements Behind 17 cm Brick Wall. . . . 37
**Figure 5.1** Average Performance of Scaling Methods Across Datasets. . . . . 39
**Figure 5.2** Evaluation Accuracy of Different Models with Different Datasets. . . . . 41
**Figure 5.3** Accuracy Vs Feature Number for Binary Classification . . . . . 42

**Figure 5.4** Confusion Matrix for All Models with Features Dataset. . . . . 44
**Figure 5.5** ROC-AUC for All Models (with 10 Features Trained Model) . . . . . 44
**Figure 5.6** Evaluation Accuracy of Different Models with Different Datasets (Action Recognition). . . . . 45
**Figure 5.7** Accuracy Vs Feature Number for Action Recognition. . . . . 45
**Figure 5.8** Confusion Matrices for Action Recognition. . . . . 47
**Figure 5.9** Confusion Matrix for Static/Movement Action Recognition. . . . . 48
**Figure 5.10** Out-of-test samples a) Multiple People. b) Different Position; 90 Degree and Back Side. c) Change Height and Angle of the Sensor, 1.5m 45 Degree. d) Laying Under Table. e) Siting Under Table. f) Furniture Obstacles Between Wall and Human. g) Laying Behind Wall. h) Non-Human Motion. 49

# LIST OF TABLES


**Table 1.1** Comparison of Sensor Technologies [**4**] . . . . . 2
**Table 2.1** Through Wall Radar in Different Applications . . . . . 7
**Table 2.2** Comparison of Industrial Sensors for Human Detection . . . . . 13
**Table 3.1** Time Domain Extracted Features . . . . . 17
**Table 3.2** Frequency Domain Extracted Features . . . . . 18
**Table 3.3** Dataset Groups . . . . . 18
**Table 4.1** Comparison of Sensors for Behind Wall Human Presence Detection . . . . . 26
**Table 4.2** Measurement Setup . . . . . 29
**Table 5.1** Sorted Combined Feature Importance . . . . . 40
**Table 5.2** Hyperparameters for Each Model . . . . . 41
**Table 5.3** Classification Report for Human Detection on 10 Features Dataset . . . . . 43
**Table 5.4** Classification Report for Action Recognition on Features Dataset . . . . . 46
**Table 5.5** Classification Report for Binary Action Recognition. . . . . 47
**Table 5.6** Multiple People Behind Wall . . . . . 50
**Table 5.7** Change Person Standing Angle and Sensor Installation Setup . . . . . 51
**Table 5.8** Obstacles Between Wall And Human . . . . . 52
**Table 5.9** Under Table Scenarios . . . . . 52
**Table 5.10** Non-Human Movement . . . . . 53
**Table A.1** Sorted Features for Action Recognition . . . . . 62

# ABSTRACT

## HUMAN DETECTION THROUGH WALLS USING FMCW RADAR SENSOR

Zainab Elfatih Mohamed MALIK

Department of Computer Engineering
Master of Science Thesis

Supervisor: Prof. Dr. Mine Elif KARSLIGİL
Co-supervisor: Asst. Prof. Ziya Cihan TAYŞİ

After an earthquake, one of the most significant challenges in rescue operations is the difficulty in locating people trapped under the rubble because they are unconscious or unable to make sounds or movements over time. In this thesis, a system has been designed and implemented to detect the presence and activities of people behind walls. In this context, data has been taken for individuals behind various types of walls and obstacles were collected using continuous wave radars (CWR) operating at 3.2 GHz, 10 GHz, and 24 GHz frequencies. A dataset was prepared, including examples of people in stationary, slow movement, and fast movement states. A total of 27 features, including statistical, time domain and frequency domain characteristics were extracted for human detection and action recognition. These features were reduced using various feature selection and extraction methods. The performance of models developed using Support Vector Machines, k-Nearest Neighbors, Decision Trees, Naive Bayes, Logistic Regression, and Random Forest methods was then evaluated. As a result, it was observed that the human detection and action recognition model developed with the Random Forest method gave the most successful results for the data collected with 24 GHz CWR sensors.

**Keywords:** Through-wall sensing, Human detection, Activity recognition, FMCW radar sensor, Machine learning.

**YILDIZ TECHNICAL UNIVERSITY**
**GRADUATE SCHOOL OF SCIENCE AND ENGINEERING**

# ÖZET

## FMCW RADAR SENSÖRÜ İLE DUVAR ARKASINDA CANLI TESPİTİ

Zainab Elfatih Mohamed MALIK

Bilgisayar Mühendisliği Anabilim Dalı
Yüksek Lisans Tezi

Danışman: Prof. Dr. Mine Elif KARSLIGİL
Eş-Danışman: Dr. Öğr. Üyesi Ziya Cihan TAYŞİ

Binaların yıkıldığı büyük depremlerden sonra göçük altındaki kişilerin kurtarılması için en önemli güçlüklerden biri göçük altındaki kişilerin bilinçlerini yitirmesi veya zaman ilerledikçe yerlerinin tespit edilmesini sağlayacak ses, hareket gibi işaretleri verememeleri sebebi ile yerlerinin tespit edilememesidir. Bu tezde, duvar arkasındaki kişilerin varlığı ve aktivitelerinin tespiti için bir sistem tasarlanmıştır. Farklı özelliklerdeki duvar arkasındaki kişilerin bilgisi 3.2 GHz, 10 GHz ve 24 GHz frekanslarında çalışan sürekli dalga radarları (continous wave radar, CWR) ile toplanarak, kişilerin durağan, yavaş ve hızlı hareket halinde olduğu örnekleri içeren bir veri kümesi hazırlanmıştır. İnsan tespiti ve hareket sınıflandırılması için istatistiksel özellikler, zamansal özellikleri ve frekans alanı özellikleri dahil olmak üzere toplam 27 özellik elde edilmiş ve bunlar farklı özellik azaltma yöntemleriyle azaltılmıştır. Daha sonra Destek Vektör Makinesi, k-En Yakın Komşuluk, Karar Ağaçları, Naive Bayes, Lojistik Regresyon ve Rastgele Orman yöntemleri ile geliştirilen modellerin başarısı değerlendirilmiştir. 24 GHz CWR algılayıcıları ile toplanan veri için Rastgele Orman yöntemi ile geliştirilen insan tespiti ve hareket sınıflandırma modelinin en başarılı sonucu vermiştir.

**Anahtar Kelimeler:** Duvar arkası algılama, Canlı tespiti, Aktivite tanıma, FMCW radar algılayıcıyı, Makine öğrenmesi.

# 1
# INTRODUCTION

## 1.1 Background

One of the biggest and most critical challenges after an earthquake is the efficient detection and rescue of trapped individuals and the presence of walls and other obstacles further complicates the task of detecting survivors [**1**]. In recent years, radar sensor technology has emerged as a promising solution to enhance post-earthquake search and rescue efforts [**2**]. Radar sensors have a wide use in various fields, including aviation, military and security due to their ability to detect objects through obstacles. The application of radar technology in search and rescue began gaining traction in the late 20th century. Within this context, Frequency Modulated Continuous Wave (FMCW) radar operates within the millimeter-wave (mmWave) spectrum (24 GHz - 100 GHz) has been particularly transformative, enabling the detection of human presence through walls and debris with high precision [**3**]. Traditional search and rescue methods often fall short in these complex environments, leading to delays that can cost lives. mmWave radar sensors offer a significant improvement by providing real-time data on the movement of individuals. Table 1.1 compares the performance of mmWave sensors with other common sensing technologies [**4**], including passive infrared (PIR) sensors, closed-circuit television (CCTV) cameras, and Trigger Radar. It highlights that mmWave sensors offer several advantages over other technologies, including the ability to penetrate non-metallic objects, excellent stability, and a longer lifespan. These features make mmWave sensors particularly suitable for through wall human detection scenarios.

## 1.2 Research Motivation

The recent earthquake on February 6, 2023, in Turkey highlighted the urgent need for better methods to find people trapped under rubble. Despite rescue efforts, finding survivors hidden behind collapsed walls remained a major challenge. Moreover in the aftermath of an earthquake, the scale of the disaster zone can be overwhelming, and the number of available rescuers is often insufficient. Which made a need for advanced technology to detect unconscious individuals in debris. This innovation could significantly enhance rescue

**Table 1.1** Comparison of Sensor Technologies [**4**]

| **Parameter** | **FMCW/mmWave Sensor** | **PIR Sensor** | **CCTV Camera** | **Trigger Radar** |
|---|---|---|---|---|
| **Induction Mechanism** | Millimeter wave radar algorithm | Thermal induction | Visible light image | Centimeter wave radar motion trigger |
| **Temperature Effect** | No | Affected if $\geq 40°C$ | No | No |
| **Penetration Ability** | Can penetrate non-metallic objects | No | No | Can penetrate non-metallic objects |
| **Working Environment** | All | Cannot work in smoke, dust, high temp | Requires good lighting | All |
| **Lifespan** | $\geq$ 10 years | $\approx$ 1000h | $\geq$ 3 years | $\geq$ 10 years |
| **Stability** | Excellent | Reduced over time | Affected by light and lens | Excellent |
| **Advantage** | Accurate, reliable | Low power, easy installation | Accurate, recording | Low cost |
| **Function** | Breath and life detection | Human presence, security alert | Security monitoring | Switch trigger, save energy |
| **Limitation** | Electromagnetic noise | Thermal noise | Privacy concerns | Poor body static measurement |

operations, ensuring that no one is left behind.

## 1.3 Problem Statement

Current methods can detect human presence behind walls but have difficulty distinguishing between activities like static, slow motion or fast motion. This distinction is vital in post-disaster rescue operations, as knowing the specific activity of trapped individuals can greatly improve the efficiency and effectiveness of rescue efforts. By integrating reliable human detection with robust activity classification, rescuers can better prioritize and respond to the needs of those trapped in collapsed structures. This project aims to address the critical need to accurately identify unconscious individuals behind wall by utilizing radar sensor technology, combined with machine learning, to enhance the detection of humans through walls and classify their activities. The primary objectives of this research are as follows:

- Evaluate the performance of millimeter wave FMCW radar sensor in detecting humans behind various types of obstacles.
- Collect and analyze practical data to assess the effectiveness of FMCW radar sensor technology.
- Develop and optimize signal processing algorithms and machine learning models to enhance the accuracy and reliability of human detection using radar data.
- Assess the practical considerations and challenges when deploying FMCW radar sensor

in real-world search and rescue missions.

The research makes several key contributions to the field of through-wall human detection using mmWave FMCW radar technology:

1. It presents a comprehensive dataset collected from controlled experiments, which can serve as a valuable resource for further research and development in this area.
2. It extracts 27 features from the radar signal, including both time domain and frequency domain features, enhancing the model's ability to detect and classify human activities.
3. It conducts extensive real scenario testing with a wide range of scenarios, including various human and non-human activities, to improve the model's robustness and generalizability.
4. It utilizes low-cost FMCW sensors, making the system more accessible and feasible for various applications.

By addressing the challenges of detecting human presence through walls, this work contributes to improving the efficiency and effectiveness of emergency response efforts, potentially saving lives in disaster situations. The findings also have broader implications for security and healthcare applications, where accurate monitoring of human activities is crucial.

Thesis is organized as follows; Chapter 1 provides an introduction and research motivation. Chapter 2 presents a comprehensive review of related literature, including studies on radar-based human detection through wall and how using machine learning can enhance the process. Chapter 3 outlines the methodology while chapter 4 contains detailed information about data collection process. It discusses the experimental setup, data collection process, signal processing techniques and machine learning models. Chapter 5 presents the results and findings of the experimental study, evaluating the performance of the FMCW radar sensors in detecting humans through various types of walls and debris with different scenarios. Chapter 6 concludes the implications of the research findings and their potential contributions to the field of search and rescue operations in addition to future work.

# 2
# LITERATURE REVIEW

## 2.1 Technologies for Human Detection Through Wall

In the aftermath of natural disasters, such as earthquakes or floods, rescuing trapped victims becomes a critical operation. Detecting and locating survivors hidden behind debris or walls is essential for efficient search and rescue efforts. Several technologies have been developed for through-the-wall human detection, each with its advantages and limitations. The most addressed techniques are followed [**5**][**6**][**7**].

(a) **Radar systems**

Radar systems are now widely recognized for their ability to detect survivors trapped under debris [**8**]. There are various types of radar, the most commonly used mentioned as fellow.

- **C**ontinuous Wave (CW) radar: CW radar emits a continuous signal and detects changes in the reflected signal caused by moving objects, including humans. It can penetrate walls and debris. Pramanik and Islam [**9**] demonstrated the use of a single-channel 24-GHz CW radar for through-the-wall detection of human heartbeats, achieving an average accuracy of 95.27% for heart rate extraction at distances ranging from 20 cm to 100 cm through wood and brick walls using maximal overlap discrete wavelet transform (MODWT). Additionally, a study [**10**] discussed the development of a short-range CW Doppler radar operating in the S-band, designed to detect humans behind visually opaque structures such as building walls.
- Frequency Modulated Continuous Wave (FMCW) radar: FMCW radar employs frequency-modulated signals to measure the range and velocity of targets, proving effective for detecting humans through walls. Ritchie et al. utilized FMCW radar for through-wall detection of human micro-Doppler. Positioned 0.5 meters outside a building, their radar effectively detected people inside by reducing wall reflection noise through digital filtering and processing micro-Doppler signatures using Singular Value Decomposition (SVD) techniques. Their classifier achieved

up to 94% accuracy in identifying individuals carrying items, indicating reliable activity recognition potential in similar scenarios [**11**]. Furthermore, a study [**12**] introduced an algorithm for non-contact vital sign detection using a 24 GHz FMCW Doppler radar, combining doppler processing and spectral estimation to accurately measure vital signs from multiple subjects within a proximity of 40 cm. The algorithm's real-time processing capabilities enable applications in remote patient monitoring and emergency surveillance.

- Stepped Frequency Continuous Wave (SFCW) radar: Similar to FMCW radar, SFCW radar provides accurate range and velocity information. It can penetrate non-metallic walls. Paper [**13**] introduces a method for detecting and classifying fine-grained human activities through walls using a stepped-frequency continuous wave bio-radar sensor. The method enhances micro-Doppler features with a new transform and uses a support vector machine for classification. Experiments showed high accuracy, achieving up to 98.78% for fixed positions and 86.67% for varying positions, improving significantly over previous methods.
- Ultra-Wide Band (UWB) radar: UWB radar emits short-duration pulses that can penetrate walls and obstacles. It is suitable for through-wall human detection. Research by Shi et al. used Ultra-Wideband (UWB) impulse radar for through-wall human detection. They proposed a method based on Convolutional Neural Network (CNN) for detecting multiple stationary human targets behind the wall. Despite the different radar technology used, this research shares the common goal of through-wall human detection, demonstrating the broad interest and varied approaches in this field [**14**].

(b) **Gas sensors**

Gas sensors can detect specific gases emitted by humans (such as carbon dioxide or ammonia) when they breathe. These sensors are less common for through-wall detection but can be useful in specific scenarios [**6**].

(c) **Robots and Drones**

Deploying robots or drones equipped with sensors such as cameras, thermal vision, or LIDAR enables remote exploration of disaster-stricken areas, facilitating the detection of human presence even through obstacles. In a study [**15**], robots are proposed for locating disaster survivors by exploring sites, detecting survivors through video and audio, and transmitting data to a cloud server while also monitoring air quality for safety. The detection models achieve high accuracy through a combined method aimed at improving results. Another research effort [**16**] introduces a framework for tracking and identifying drones using millimeter-wave radar. The system processes signals to distinguish targets and employs a convolutional neural network for recognition, achieving high accuracies of

98.4% and 98.1% for one and two targets, respectively. Additionally, the study uses radar micro-Doppler to detect and classify small drones for security purposes. A deep learning classifier effectively discriminates between drones and birds as well as different types of drones, demonstrating significant performance enhancement compared to previous methods [**17**].

(d) **Acoustic / Seismic**
Acoustic sensors detect sound waves generated by human movement or breathing. Seismic sensors pick up ground vibrations caused by footsteps or other activities. These sensors can work through walls but may be affected by environmental noise [**6**].

(e) **Infrared (IR)**
IR sensors detect thermal radiation emitted by objects, including humans. They can operate through walls, but accuracy depends on the material and thickness of the barrier [**6**].

## 2.2 Importance and Applications of Through-Wall Human Detection

Through-wall human detection (TWHD) has become increasingly significant due to its wide range of applications. Below are some of its applications [**9**][**14**][**18**].

- Emergency Rescue: TWHD can play a pivotal role in locating survivors in disaster-stricken areas, such as earthquake sites or collapsed buildings. This can significantly enhance the efficiency of rescue operations and potentially save lives.
- Healthcare and Elderly Monitoring: TWHD can be used to monitor the health and activities of elderly or disabled individuals. This can provide real-time health status updates and alert caregivers in case of emergencies.
- Security and Anti-Terrorism: TWHD can be used for security purposes, such as detecting intruders or potential threats behind walls. This can enhance the effectiveness of security systems and contribute to public safety.
- Military Reconnaissance: In military operations, TWHD can provide crucial information about enemy activities behind walls or barriers. This can give strategic advantages and contribute to mission success. These applications underscore the importance of TWHD in various domains, from public safety and healthcare to military operations. The development and refinement of this technology can have far-reaching impacts on society and individual lives.

## 2.3 Radar Sensor Technology in Through Wall Applications

Radar technology plays a crucial role in various applications, enabling the detection of the velocity of moving targets. Radar technologies provide valuable information about the motion of objects within the radar's field of view. To gain a comprehensive perspective on the field of through wall, a comparative analysis table has been prepared for the latest studies that uses radar technology in through wall applications. Table 2.1 summarizes various studies, each identified by its reference and publication year, radar type used, the operating frequency, the type of wall, the wall thickness and the specific application for which the radar system is implemented. This comparison aims to provide valuable insights into the recent through-wall radar technology, particularly in scenarios involving human detection.

**Table 2.1** Through Wall Radar in Different Applications

| **Ref./Year** | **Radar Type** | **Freq. (GHz)** | **Wall Type** | **Wall Thick-ness (cm)** | **Application** |
|---|---|---|---|---|---|
| [**19**] 2022 | UWB | 0.4 | Standard brick wall | 40 | Human targets detection |
| | | | Mix wall | 90 | |
| | | | Actual ruin | - | |
| [**20**] 2021 | SFCW | 1.6 - 2.2 | Brick wall | 24 | Human counting |
| [**21**] 2021 | UWB | 0.38 - 4.4 | - | 30 | Human motion detection |
| [**22**] 2018 | UWB | 0.4 | Mix wall of brick, reinforced concrete and wood | 100 (30,40,30) | Vital detection |
| [**23**] 2023 | UWB | 0.4 ± 0.02 | Brick wall | 30 | Multi-target localization and Vital sign detection |
| [**24**] 2021 | Micro-Doppler Signatures | 0.38 - 3.4 | Concrete wall | 30 | Human motion detection |
| [**25**] 2018 | IR-UWB | 0.4 | Mix wall | 100 | Human respiratory move-ments |
| [**26**] 2019 | Micro-Doppler | 2.4 | glass | 0.8 | Human motion detection |

**Table 2.1** Through Wall Radar in Different Applications (continued...)

| Ref./Year | Radar Type | Freq. (GHz) | Wall Type | Wall Thick-ness (cm) | Application |
|---|---|---|---|---|---|
| [**27**] 2023 | UWB | 8 - 10 | standard building materials, such as brick, wood etc. | At least 25 | Aftermath victim detection |
| [**28**] 2020 | Multichannel Doppler Radar | 2.49 | Brick wall | 15 | Human subject localization and respiration rate detection |
| | | | Glass sheet | 2 | |
| | | | Wood sheet | 2 | |
| [**29**] 2019 | SFCW | 2 - 4 | Plastered brick wall | 13.5 | Classification of Human Posture |
| [**30**] 2023 | UWB bio-radar | 7.29 | four layers of thick gypsum board | 1.5 each | Post-Disaster Compression state of Injured Individuals |
| [**31**] 2021 | UWB | 1.6 – 2.2 | Six gypsum boards with a height of 2.00 m, width of 1.20 m | 1 | Human motion recognition |
| [**32**] 2019 | Non-contact Doppler sensor | 2.4 | Solid building grade bricks placed on top of | 5 | Identify humans trapped under debris |
| | | | Thick wooden board and | 0.5 | |
| | | | Thinner wooden board | 0.2 | |
| [**33**] 2022 | CW Doppler Radar | 15 | - | 20 | Human body detection |
| [**34**] 2022 | doppler | 2.4 | Solid building grade bricks placed on top of | 5 | Detection of cardiopulmonary activities of trapped humans in Rescue Relief Events |
| | | | Thick wooden board and | 0.5 | |

**Table 2.1** Through Wall Radar in Different Applications (continued...)

| Ref./Year | Radar Type | Freq. (GHz) | Wall Type | Wall Thick-ness (cm) | Application |
|---|---|---|---|---|---|
| | | | Thinner wooden board | 0.2 | |
| [**35**] 2019 | UWB | 2.9 - 10.1 | - | 25 | Detection of vital signs |
| [**37**] 2021 | UWB MIMO imaging radar | 1.75 - 2.25 | Bricks wall | 12 | Multi-Subject Localization and Vital Signs Monitoring |
| [**38**] 2023 | UWB MIMO | 1 | - | 37 | Multi-target detection |
| [**39**] 2021 | IR-UWB | 1.5 - 6 | Layer of wood block, clay brick, and cement brick wall | - | Human respiration detection With hovering drone |
| [**40**] 2019 | IR-UWB | 7.29 | - | 30 | Heartbeat frequency detec-tion |
| [**41**] 2022 | Random Code Radar Sensor With Multi-Domain Feature Fusion | 1.5 | Brick wall | 20 | Human motion recognition |
| [**42**] 2019 | Doppler Radar | 7.25 | Thick wooden panel | 0.6 | Human voice recognition |
| [**43**]2018 | SFCW | 4 - 6 | Thick ply-wood wall | 1.2 | Human signature detection |
| [{**44**}] 2023 | TWR | 3 | Standard wall | 10 + 5 air gap | Multi-object locating |
| [**45**] 2021 | telescopic SIMO UWB radar | 40 | - | 20 | Detection and localization for multiple human subjects |

**Table 2.1** Through Wall Radar in Different Applications (continued...)

| Ref./Year | Radar Type | Freq. (GHz) | Wall Type | Wall Thick-ness (cm) | Application |
|---|---|---|---|---|---|
| [**46**] 2021 | Microwave Detection radar | 1.2 | - | 30 | Respiration rate of a living human hidden behind an inhomogeneous optically opaque medium |
| [**47**] 2019 | Cross-Correlation of Dual-Station SFCW Radars | 1.6 - 2.2 | Solid brick wall | 20 | Detection and Localization for Multiple Stationary Human Targets |
| [{**48**}] 2020 | through-wall radar imaging | 0.9 | - | 10 | Through-wall radar imaging |
| [**49**] 2022 | UWB on-line-of-sight (NLOS) Signals | 6 - 8.5 | double-glazing (only static case) | 10 | Human detection |
| | | | Wooden door | 3 and 5 | |
| | | | Brick wall | 15 | |
| | | | Glass window | 2 | |
| [**50**] 2020 | Self-Injection-Locked (SIL) radar Technology | 0.433 | Thick concrete wall | 35 | Life detector |
| [**51**] 2022 | UWB | 6 - 8.5 and 7.25 - 10.20 | Standard wall | 10 - 35 | Human detection |
| [**52**] 2023 | FMCW | 60-64 | Glass | 0.5 | Human detecrion |
| | | | Concrete wall | 10 | |
| [**53**] 2022 | FMCW | 24 | Brick wall | 20 and 40 | Detecting Respiration Vital Sign |
| [**54**] 2023 | FMCW | 24 | Brick wall | 20 | Clutter Reduction in Detecting Trapped Human Respiration |
| This work | FMCW | 24 | Wood | 3-4 cm | Human detection and action recognition |
| | | | brick | 17 cm | |

#### 2.3.0.1 Wall Consideration and Radar Frequency

Walls show varying degrees of transparency to radar waves depending on their material type and thickness. Different wall materials, such as concrete, brick, wood, or drywall, possess unique electromagnetic properties that influence how radar waves propagate through them. Regarding wall consideration and radar frequency, [**33**] concludes their experiment when dealing with 15 GHZ thorough walls radar system, as the wall considerably attenuates the electromagnetic wave, making the detection of heartbeat signals challenging. However, the system remains capable of detecting human respiration signals in such conditions. Moreover, [**36**] addresses that the findings validate that the thickness of the obstacle has a direct impact on the detected signal level and the depth position. A thicker obstacle leads to increased attenuation and phase shift, whereas a thinner obstacle results in the opposite effect. Figure 2.1 expresses the distribution of literature for radar frequency value and the wall thickness. It includes a diverse range of radar types such as UWB, SFCW, and FMCW, each with varying capabilities to penetrate different wall materials and thicknesses.

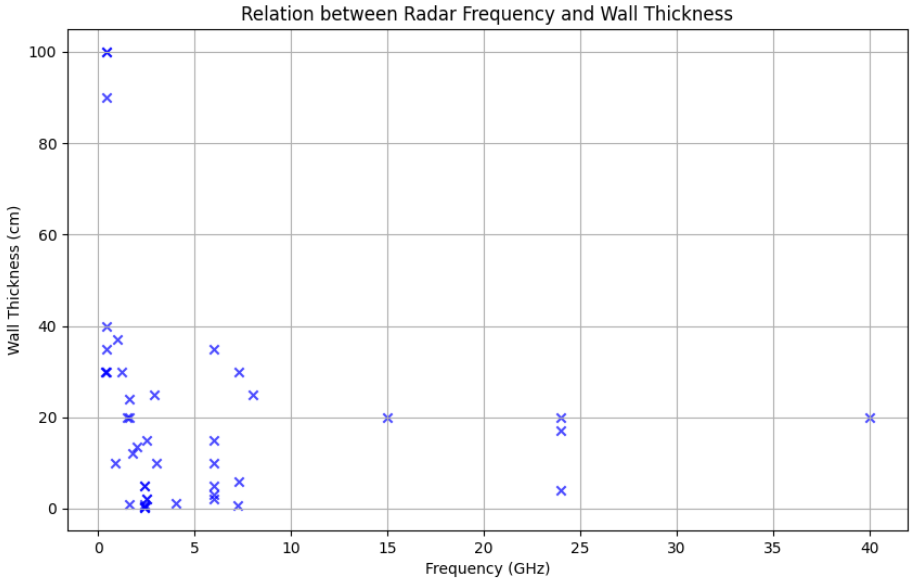



**Figure 2.1** Frequency Vs. Wall Thickness Distribution in Literature

In addition to that [**55**] reviewed many literatures that addressed five key tasks: estimating Breathing Rate (BR), Heart Rate (HR), the distance between the victim and the radar, the number of humans within the scanned area, and detecting human presence using UWB, SFCW and FMCW radars. Among these, BR estimation is the most frequently examined, with UWB radar sensors being the preferred choice. The reviewed studies show that wall thickness varies from 0.15 m to 1 meter, using standard materials like brick, wood, and concrete. A 0.4 GHz emission frequency is effective for detecting BR, HR, and distance through walls up to 1 m thick. In contrast, radars emitting at 7-10 GHz can penetrate walls up to 40 cm thick but have a limited detection range of 5 m, with accurate vital sign detection

generally up to 3 m. Moreover, radars with more than 10 GHz can detect nonmetallic walls with around 0.2 – 0.3 meters within distance less than 5 meter. Most methods use the frequency domain to detect target metrics, extracting BR and HR by identifying the dominant frequency for short distances. For longer distances or low signal-to-noise ratio scenarios, sophisticated algorithms like arctangent demodulation, ensemble empirical mode decomposition-based frequency accumulation, discrete wavelet transform, convolutional neural networks, and variable mode decomposition are employed, achieving high accuracy across tasks.

## 2.4 Machine Learning for Human Detection Through Wall

In [**56**] utilizing UWB sensors for multi-status target identification, features such as kurtosis, skewness, energy, maximum amplitude, variance, and covariance were extracted. The dataset included 300 samples for training and verification, with 50 samples per status. The fuzzy pattern recognition algorithm achieved accuracies of 98% for no person, 82% for normal breathing, 96% for swing arms, 94% for two-person normal breathing, and 96% for two-person walking 2 meters away. Another study [**57**] focused on UWB NLOS for human detection, extracting features such as max, min, mean, standard deviation, skewness, kurtosis, energy, max/min, max–min, SD/mean, and (max–min) squared. The raw data points for static case totaled 23,552 samples each of them with 256 window size while for dynamic case totaled 17,408 samples each of them with 256 window size. The LSTM model achieved 99.70% accuracy for static mode and 94.83% for dynamic mode. In a different study [**58**] using UWB sensors for human detection, 500 groups of pulses were taken from each state with 1000 pulse-sampling points. Accuracies reached 95.2% for the autoencoder, 96.4% for the stacked denoising autoencoder, and 94.8% for the sparse autoencoder. A recent study employed raw radar data for human detection with a dataset totaling 2 hours. The TWP-CNN model achieved 88.24% accuracy, FCN+DAFE achieved 75.64%, and improved U-Net + DAFE achieved 52.49% [**59**]. Another study [**60**] using TWR for object detection and classification reported accuracies of 97% with the KNN method and 99% with the CNN method using time series data. The paper [**62**] discusses a low-cost, lightweight UWB radar sensor named X4M200 by Novelda, operating in the X-band (8.0 - 10 GHz) frequency range. The study utilized a dataset of 9,768 samples in a 6 x 6 sec window, including 823 samples indicating no human presence. The wall types included brick wall (10-35 cm) and wooden door with proposed distances 1-5 meter between the sensor and the victim. The proposed solution combines a visual sensor with UWB radar and applies deep learning algorithms for human detection and respiration monitoring. The method achieved over 99% accuracy in detecting human presence in indoor environments and maintained an average distance detection error of less than 0.28 meters across different scenarios, including outdoor, indoor without obstacles, and indoor with obstacles like brick walls and wooden doors. In a study [**61**] using SFCW for human detection and

classification based on raw radar signals. The experiments were conducted through two types of walls: a brick wall and a drywall. The brick wall, plastered, consists of standard bricks with a thickness of 135 mm and an approximately 10 mm thick plaster layer that is not homogeneous. The drywall was created by placing five pieces of 12.5 mm thick plates side-by-side, with a nonhomogeneous air gap of less than 10 mm between the plates. The CNN method achieved accuracies of 97% through a brick wall and 98.56% through drywall. These studies collectively demonstrate the effectiveness of various machine learning and deep learning models in human detection through walls, showcasing robust performance and high accuracies across different sensor types and feature extraction techniques. Specifically, LSTM and CNN models have shown superior performance in static and complex scenarios, respectively, underscoring their potential for practical applications in security, surveillance, and rescue operations.

## 2.5 Commercially Available Industrial Sensors for Human Detection

Commercially available industrial sensors for human detection vary widely in terms of cost, size and portability, power requirements, and complexity of the installation process. Generally, these factors influence the choice of sensor based on specific application needs. Table 2.2 shows a comparison of different sensors with their prices and features.

**Table 2.2** Comparison of Industrial Sensors for Human Detection

| Sensor Name | Range (meters) | Frequency (GHz) | Cost (USD) |
|---|---|---|---|
| UWB P440, UWB P410 [**56**, **57**] | 10 | 3.1-4.8 | ~5K |
| N9916A [**78**] | 14 | - | ~21K |
| YSR120 [**79**] | 12 | 0.6-1.8 | ~20K |
| XAVER400 [**80**] | 20 | 3-10 | ~47K |

In this work, we used the 24GHz mmWave Sensor - Human Static Presence Module Lite (MR24HPC1). This sensor offers a 5-meter detection range, operates at a 24 GHz frequency, and is cost-effective at just 12 USD.

# 3
# METHODOLOGY

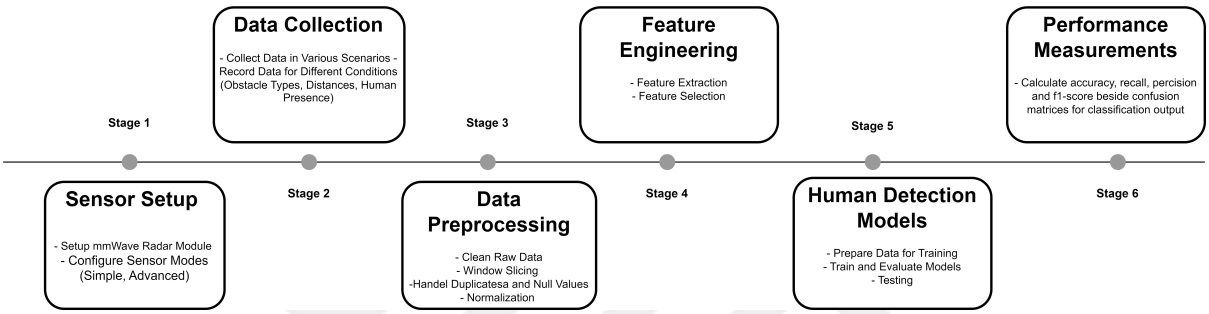



**Figure 3.1** System Overview.

This project aims to detect human under trapped areas and to enhance search and rescue operations by employing Frequency-Modulated Continuous-Wave (FMCW) radar sensor technology and machine learning techniques. The goal is to improve the detection of humans through walls and accurately classify their activities, such as moving fast, moving slow, or remaining static. By leveraging advanced sensing and classification methods, the project seeks to provide more efficient and reliable tools for locating and identifying individuals in disaster scenarios. Ultimately, this could significantly aid in saving lives and improving rescue mission outcomes. The system contains a main six-stage for utilizing a 24 GHz mmWave FMCW radar sensor for human presence detection as shown in Figure 4.1. The first stage, Sensor Setup, involves setting up the mmWave radar module and configuring the sensor modes for both simple and advanced settings. In the second stage, Data Collection, data is gathered in various scenarios, recording under different conditions such as obstacle types, distances, and human presence to build a comprehensive dataset. The third stage, Data Preprocessing, involves cleaning the raw data, slicing it into windows, handling duplicates and null values, and normalizing it to prepare for feature extraction. During the fourth stage, Feature Engineering, essential features are extracted from the preprocessed data, identifying and selecting the most relevant ones for accurate human presence detection and activity classification. The fifth stage, Human Detection Models, involves preparing the data for training and training the detection models beside testing to ensure reliable detection of human presence and activity classification in various scenarios. Finally, performance measurements. Each stage is crucial for developing

and implementing an effective human presence detection system using the mmWave FMCW radar sensor.

## 3.1 Preprocessing

The aim of preprocessing is to prepare raw data for human detection models. This involves handling null values and removing duplicate entries to ensure data integrity. Besides that, window slicing, and feature scaling are also applied to the data. These steps create a clean, consistent, and well-structured dataset, improving the performance and accuracy of human detection models.

### 3.1.1 Window Slicing

In this study, the majority of the signal data was recorded over durations ranging from 2 to 5 minutes, resulting in approximately 200 to 600 time series data points per signal with 0.5 second sampling rate. To ease the processing and analysis of these signals, we implemented a data window slicing technique. This method involves segmenting each signal into smaller windows. After processing window slicing, there is 208 signals labeled as no human (class 0), while 348 instances were labeled as human (class 1) exist putting into consideration that human exist class encompass various motion categories, including static, slow, and fast motion, indicating the diversity within this classification.

### 3.1.2 Feature Scaling

Feature scaling is a crucial sub-step in the preprocessing phase, as it can significantly impact classification results. These scaling techniques help improve the performance of machine learning algorithms by ensuring that each feature contributes equally and helps prevent numerical instability. In this thesis mean normalization scaling, standardization and minimum – maximum (min-max) scaling methods are used and applied to human detection models and average accuracy calculated to determine the best method.

- Mean Normalization Scaling transforms the data such that the mean of each feature becomes 0. It centers the data around the mean.

$$x' = \frac{x - \mu}{x_{\text{max}} - x_{\text{min}}} \tag{3.1}$$

  Where: x' is the normalized value, x is the original value, $\mu$ is the mean of the feature, $x_{\text{max}}$ is the maximum value of the feature and $x_{\text{min}}$ is the minimum value of the feature.

- Standardization transforms the data to have a mean of 0 and a standard deviation of 1.

$$x' = \frac{x - \mu}{\sigma} \tag{3.2}$$

  Where: x' is the standardized value, x is the original value, $\mu$ is the mean of the feature and $\sigma$ is the standard deviation of the feature.

- Min-Max Scaling transforms the data to fit within a specific range, typically [0, 1].

$$x' = \frac{x - x_{\text{min}}}{x_{\text{max}} - x_{\text{min}}} \tag{3.3}$$

  Where: x' is the scaled value, x is the original value, $x_{\text{max}}$ is the maximum value of the feature and $x_{\text{min}}$ is the minimum value of the feature.

## 3.2 Feature Engineering

Variety of features have been collected to enhance the accuracy of human detection behind walls using sensors. The primary features are time series values (64 values) representing the motion energy between 0 - 250 detected by the sensor, which captures the dynamic changes in movement over time. Additionally, various contextual features, including wall type, wall thickness, the height of the sensor installation height and the distance between the wall and the target labeled with the presence or absence of a person, as well as the nature of their movement, whether they are moving fast, moving slow, or remaining static. These comprehensive features allow for robust analysis and improve the precision of human activity classification behind walls.

### 3.2.1 Feature Extraction

Feature extraction and selection are critical steps in signal classification, as they involve identifying and choosing the most relevant attributes of the signal that contribute to accurate and efficient classification. Extracting features transforms raw signal data into a more informative and compact form, which is easier for machine learning algorithms to process and interpret. The features extracted from a signal can be broadly categorized into time domain, and frequency domain features. Time domain features are explained in table 3.1 which provides a general summary of the signal's amplitude and distribution characteristics. Frequency domain features are explained in Table 3.2 which reveals the signal's behavior in terms of its frequency components and energy distribution.

Where: $x$ is the signal, $N$ is the number of samples in the signal, $x_i$ represents the $i$-th sample, $\max(x)$ and $\min(x)$ denote the maximum and minimum values of the signal respectively, $\mu$

**Table 3.1** Time Domain Extracted Features

| Feature | Description | Equation |
|---|---|---|
| Maximum value | The highest value in the signal. | $\max(x)$ |
| Minimum value | The lowest value in the signal. | $\min(x)$ |
| Mean value | The average value of the signal. | $\mu = \frac{1}{N}\sum_{i=1}^{N} x_i$ |
| Median | The middle value in the sorted order of the samples. | $x_{(\frac{n+1}{2})}$ |
| Standard deviation | A measure of the signal's spread or dispersion. | $\sigma = \sqrt{\frac{1}{N}\sum_{i=1}^{N}(x_i - \mu)^2}$ |
| Skewness | The asymmetry of the signal distribution. | Skewness $= \frac{\frac{1}{N}\sum_{i=1}^{N}(x_i-\mu)^3}{\sigma^3}$ |
| Kurtosis | The peak sharpness of the signal distribution. | Kurtosis $= \frac{\frac{1}{N}\sum_{i=1}^{N}(x_i-\mu)^4}{\sigma^4} - 3$ |
| Variance | The measure of signal variability. | $\text{Var}(x) = \frac{1}{N}\sum_{i=1}^{N}(x_i - \mu)^2$ |
| Signal's energy | The sum of the squared values of the signal. | $E = \sum_{i=1}^{N} x_i^2$ |
| Max/Min ratio | The ratio of the maximum value to the minimum value of the signal. | $\frac{\max(x)}{\min(x)}$ |
| Max-min difference | The difference between the maximum and minimum values of the signal. | $\max(x) - \min(x)$ |
| Standard deviation-mean ratio | The ratio of the standard deviation to the mean value of the signal. | $\frac{\sigma}{\mu}$ |
| Squared difference (max and min) | The square of the difference between the maximum and minimum values of the signal. | $(\max(x) - \min(x))^2$ |
| Root mean square (RMS) | The square root of the mean of the squares of the signal values. | $\text{RMS} = \sqrt{\frac{1}{N}\sum_{i=1}^{N} x_i^2}$ |
| Turns count | The number of times the signal changes direction. | $\sum_{i=2}^{N-1} [\text{I}(x_{i-1} - x_i)(x_i - x_{i+1})$ |
| Mobility | The square root of the first derivative's variance divided by the signal's variance. | $\text{Mobility} = \sqrt{\frac{\text{Var}(\Delta x)}{\text{Var}(x)}}$ |
| Form factor | The ratio of RMS to the average value of the signal. | $\frac{\text{RMS}}{\mu}$ |
| Entropy | The measure of uncertainty or randomness in the signal. | $H = -\sum_{i=1}^{N} p_i \log p_i$ |
| Power | The sum of absolute squares of samples divided by signal length. | $P = \frac{1}{N}\sum_{i=1}^{N} \lvert x_i \rvert^2$ |

is the mean value, $\sigma$ is the standard deviation, $\Delta x$ is the first derivative of the signal, $\text{Var}(x)$ represents the variance of the signal, $\text{med}(x)$ represents the median of the signal, $E$ is the energy of the signal, RMS is the root mean square, $I$ is the indicator function, $p_i$ is the probability of the $i$-th value, $H$ is the entropy, and $P$ is the power of the signal.

Where Pi is the power at frequency component i, N is the frequency components, $f_i$ is the frequency of the i-th component and $P_cum$ is the cumulative power. After extracting features, three distinct datasets are here as shown in Table 3.3 The features dataset has been used in this thesis for human detection.

**Table 3.2** Frequency Domain Extracted Features

| Feature | Description | Equation |
|---|---|---|
| Total Power | Distribution of power into frequency components in the frequency domain. | $P_{\text{total}} = \sum_{i=1}^{N} P_i$ |
| Spectral Moments | Statistical measures describing the distribution of frequency components: mean frequency, median frequency, frequency variance, frequency skewness. | • Mean Frequency: $f_{\text{mean}} = \frac{1}{N}\sum_{i=1}^{N} f_i P_i$<br>• Median Frequency: $f_{\text{median}} = f_{\left(\frac{N+1}{2}\right)}$<br>• Frequency Variance: $\sigma_f^2 = \frac{1}{N}\sum_{i=1}^{N}(f_i - f_{\text{mean}})^2 P_i$<br>• Frequency Skewness: $\gamma_f = \frac{1}{N}\sum_{i=1}^{N}\left(\frac{f_i - f_{\text{mean}}}{\sigma_f}\right)^3 P_i$ |
| Shannon Entropy | Measure of spectral power distribution, indicating the uncertainty or variability in the signal's energy distribution across different frequencies. | $H = -\sum_{i=1}^{N} \frac{P_i}{P_{\text{total}}} \log\left(\frac{P_i}{P_{\text{total}}}\right)$ |

**Table 3.3** Dataset Groups

| Dataset name | Dataset explanation |
|---|---|
| Raw time domain dataset | Time-domain representation of the signal without any transformation. |
| Raw frequency domain dataset | Frequency-domain representation of the signal without any transformation. |
| Feature dataset | Dataset containing features derived from the time domain, such as statistical measures (mean, variance, etc.) and features derived from the frequency domain, such as total power, spectral moments, etc. |

### 3.2.2 Feature Selection

By selecting the most relevant features from the features above, the performance of signal classification algorithms can be improved. Effective feature selection reduces the dimensionality of the data, minimizes overfitting, and enhances the generalization capability of the classification model. In this thesis three methods are used in order to make robust feature selection. Then the median score is calculated and ranked according to it providing a robust consensus on feature importance.

- Information Gain: This method evaluates the worth of an attribute by measuring the information gain with respect to the class. Information gain is based on the decrease in entropy after a dataset is split on an attribute. It helps in identifying which features provide the most useful information for classification.
- Recursive Feature Elimination (RFE): RFE works by recursively removing attributes and building a model on those attributes that remain. It uses model accuracy to identify

which attributes (and combination of attributes) contribute the most to predicting the target attribute.

- Random Forest: This is an ensemble method that can be used for feature selection by looking at the importance scores of the features. In random forests, each tree in the ensemble is built from a sample drawn with replacement from the training set. Feature importance is calculated based on how much each feature decreases the weighted impurity in a tree, which is averaged over all trees in the forest.

#### 3.2.2.1 Correlation

In the context of feature extraction, correlation is crucial for several reasons,

- It can be used to detect periodicities and repeating patterns within a signal.
- Correlation analysis can help in noise reduction by identifying and separating noise.

Below is correlation matrix visualization for all features. Figure 3.2 shows correlation matrix, which is a table showing correlation coefficients between variables. Each cell in the matrix shows the correlation between two variables. The value is between -100 and 100, where:

- 100 indicates a perfect positive correlation.
- 0 indicates no correlation.
- -100 indicates a perfect negative correlation.

Darker shades of red represent stronger positive correlations. The diagonal line of 100s represents the perfect correlation of each variable with itself. This matrix helps to identify which variables have strong or weak correlations and is useful in statistical analysis to determine potential relationships between variables. In addition, Figure 3.3 gives more detailed information with scatterplot matrix. It showcases a series of relationships between pairs of variables, with each plot providing insights into how one variable may vary from another.

## 3.3 Human Detection Models

Human detection behind walls is a challenging task due to the occlusion and interference caused by the wall material. To address this, we leverage a combination of motion energy time series data and contextual features such as wall thickness, sensor height, and installation height. The goal is to accurately classify human presence and movement behind walls using

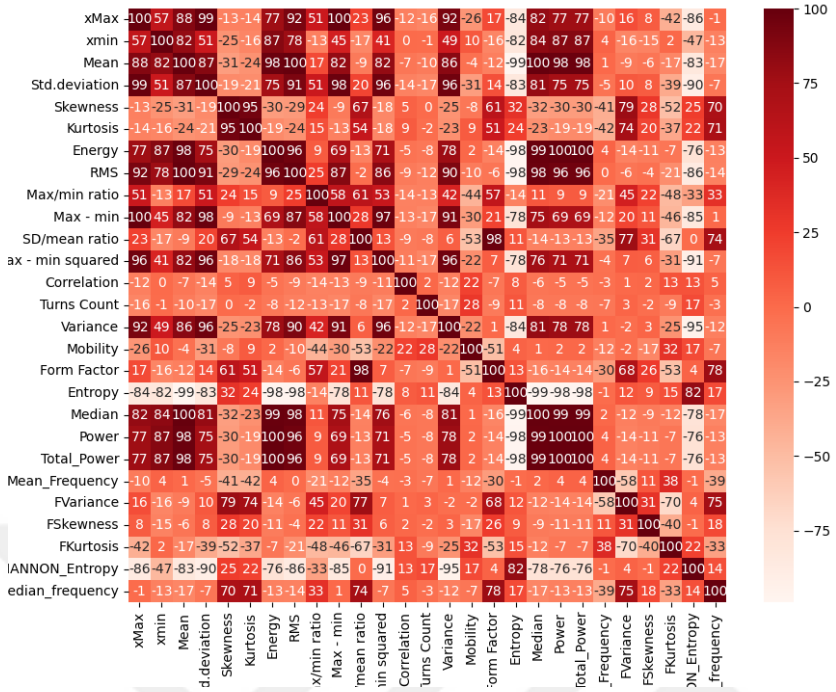



**Figure 3.2** Correlation Matrix.

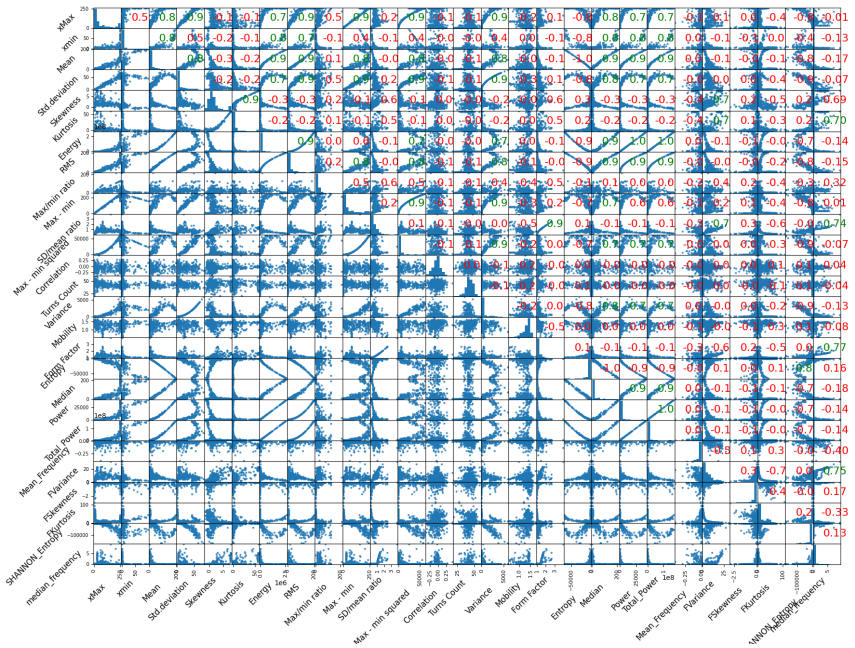


**Figure 3.3** Scatter Matrix

advanced machine learning techniques. The dataset collected includes labels indicating the presence or absence of a person, and the type of movement (e.g., moving fast, moving slow, or static). In this study, various machine learning and deep learning methods were employed

to improve human detection accuracy behind walls. Each method has unique characteristics and advantages, making them suitable for different aspects of the task. To effectively build a classification model, the dataset is typically divided into three subsets: training, validation, and testing. The training set contains labeled data used to construct the model, which is then used to make predictions on the test set and the validation subset is used to evaluate the performance of a model during training. Common ratios for train/test split are 80/20, 70/30, or 60/40. The validation set is typically chosen from the training set. The data is first divided into training and testing sets, following the common split ratios mentioned above. After this initial split, a portion of the training set is further divided to create the validation set.

Cross-validation is a technique used to ensure a more robust evaluation of the model, particularly useful with smaller datasets. Instead of having a single validation set, the data is split into multiple subsets, and the model is trained and validated multiple times, each time using a different subset as the validation set and the remaining data as the training set. The most common type of cross-validation is k-fold cross-validation where the training set is divided into k subsets (folds). The model is trained on k-1 folds and tested on the remaining fold, repeating this process until each fold has been used as a test set. This results in k models, and their average is used to create the final model. Generally, smaller datasets use more folds, while larger datasets use fewer folds. In this study, the dataset was randomly split into 80% training and 20% test sets. A 5-fold CV was applied to the training set, and the final model's accuracy was evaluated based on its predictions on the test set.

In this study, various machine learning and deep learning methods were employed to improve human detection accuracy behind walls. Each method has unique characteristics and advantages, making them suitable. Below is a brief explanation of the methods used:

- Support Vector Machine (SVM) SVM is a supervised learning algorithm used for classification tasks. It works by finding the hyperplane that best separates the data into different classes. SVM is particularly effective in high-dimensional spaces and is robust to overfitting, especially in cases where the number of dimensions exceeds the number of samples [**72**].
- k-Nearest Neighbors (kNN) kNN is a simple, instance-based learning algorithm that classifies a data point based on the majority class among its k-nearest neighbors in the feature space. It is intuitive and easy to implement but can be computationally expensive as it requires calculating the distance between the query and all training samples [**73**] .
- Logistic Regression (LR) LR is a statistical method used for binary classification. It models the probability that a given input belongs to a particular class. Despite its simplicity, LR is powerful for linearly separable data and provides a probabilistic framework for classification [**74**].

- Naïve Bayes (NB) Naïve Bayes is a simple, probabilistic classifier based on Bayes' theorem, which assumes that features are independent given the class. Naïve Bayes performs well in many applications, it is computationally efficient and effective, making it a popular choice for initial models and baseline comparisons[**75**].

- Decision Tree (DT) A Decision Tree is a classification and regression algorithm that splits the data into subsets based on feature values, forming a tree-like structure of decisions. Each node represents a feature, each branch a decision rule, and each leaf a class label or output. Decision Trees are easy to interpret and visualize but can overfit the data [**76**].

- Random Forest (RF) RF is an ensemble learning method that builds multiple decision trees during training and outputs the mode of the classes for classification tasks. It is highly effective for a variety of tasks due to its ability to handle large datasets with higher dimensionality and mitigate overfitting [**77**].

# 4
# DATA COLLECTION

In this chapter, we discuss the data collection process for detecting human presence behind walls using Frequency Modulated Continuous Wave (FMCW) radar. We explored various sensors to find the most effective one for this task. Ultimately, we chose the Seeed Studio 24GHz mmWave Sensor - Human Static Presence Lite Module (MR24HPB1) due to its high sensitivity and robustness against environmental interferences. The purpose of data collection is to gather diverse and comprehensive datasets that will allow us to train, validate, and test our machine learning models effectively. These datasets are crucial for developing a reliable system that can accurately detect and classify human activities behind walls in real-world scenarios.

## 4.1 FMCW Working Principle

The Frequency Modulated Continuous Wave (FMCW) radar operates on a unique principle that sets apart from traditional pulsed radar systems. Unlike pulsed radar, which sends out strong pulses, FMCW radar emits a continuous wave with a slowly changing frequency over time, modulated in a saw-like or triangle-shaped pattern. As shown in Figure 4.1 the signal travels through space until it encounters a target, at which point it reflects back toward the radar system. The reflected signal's frequency changes based on the target's distance and velocity, with the difference in frequency between the sent and received signals providing information about the target's speed [**63**] [**64**].

By measuring the time, it takes for the signal to travel to the target and back, the radar calculates the distance to the target, with longer travel times indicating greater distances. FMCW radar continuously emits a signal, and its dynamic modulation makes it useful across various applications like human activity recognition [**65**][**66**][**67**], healthcare application [**63**][**68**].

## 4.2 Sensor Overview

Multiple sensors, including 3.2 GHz and 10 GHz CW radar sensors, were tested, and the 24 GHz FMCW sensor was selected for its good ability to detect human presence behind wall.

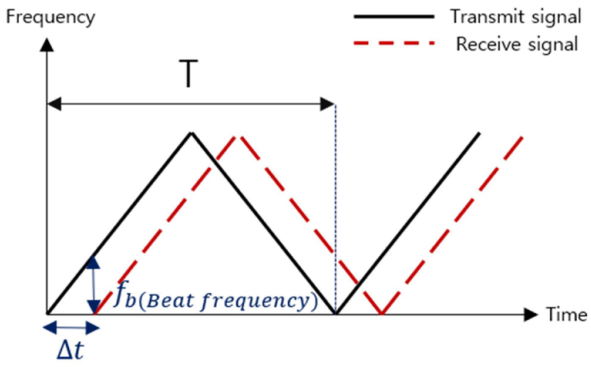



**Figure 4.1** FMCW Signal Pattern

Table 4.1 provides a comparison of various sensors evaluated for detecting human presence, highlighting their frequency, capabilities, and output formats.

1. **HB100 Doppler Radar Sensor**: This sensor operates at a frequency of 10 GHz and has a range of up to 3 meters for detecting human micro and normal motion. However, it struggles with behind-wall scenarios. Figure 4.2 shows testing experiments.

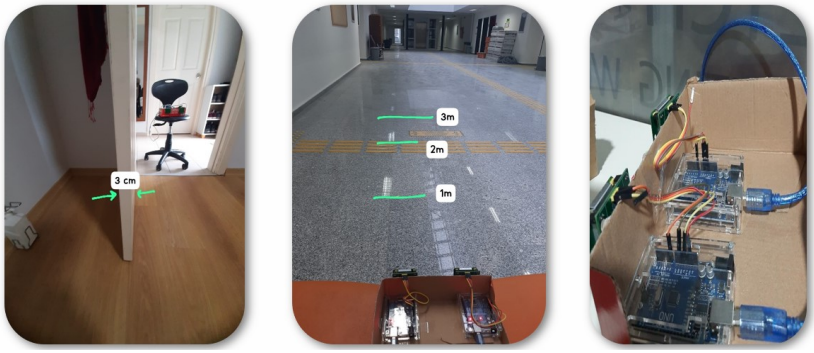



**Figure 4.2** HB100 Testing Experiments

2. **RCWL-0516 Continuous Wave Sensor**: This sensor operates at 3.12 GHz and outputs a digital signal. To obtain an analog output, a wire is connected to pin 12 on the sensor IC chip. It can detect motion through walls of various thicknesses but struggles with detecting small or micro motions. Figure 4.3 shows testing experiments for RCWL sensor beside the output signals. Figure 4.4 shows Testing environment for the sensor, to test sensor behind wall there is a need to go through different thicknesses and materials to check the effectiveness.

3. **Seeed Studio Sleep Motion Detection Sensor**: This sensor can detect micro motion but cannot detect through walls.

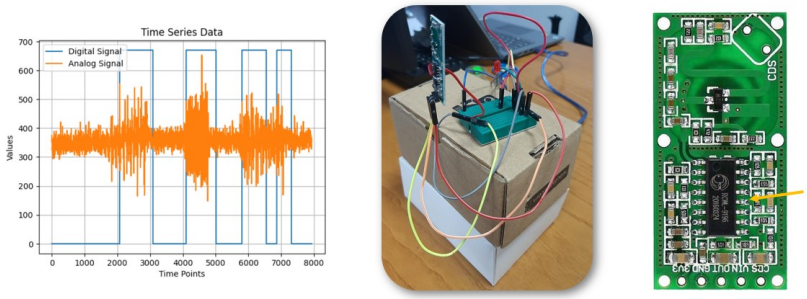



**Figure 4.3** RCWL 0516 Testing Experiments

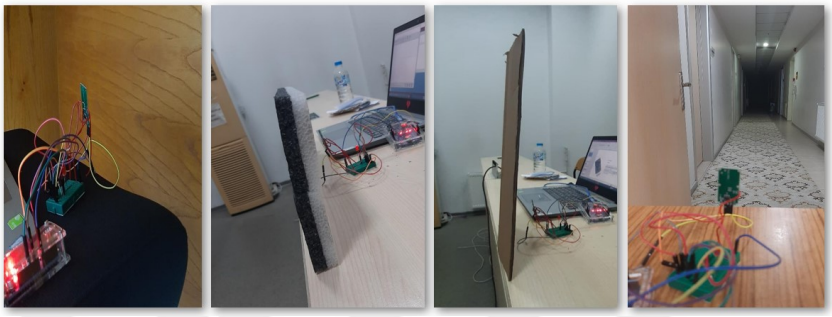


**Figure 4.4** RCWL 0516 Testing Environment

4. **Seeed Studio Human Detection Module**: This sensor can detect small and micro motions through obstacles, but it provides processed data as output. Having raw data is crucial for this project to accommodate different scenarios. Figure 4.5 shows the output dataframe from the sensor when interfacing with Arduino.

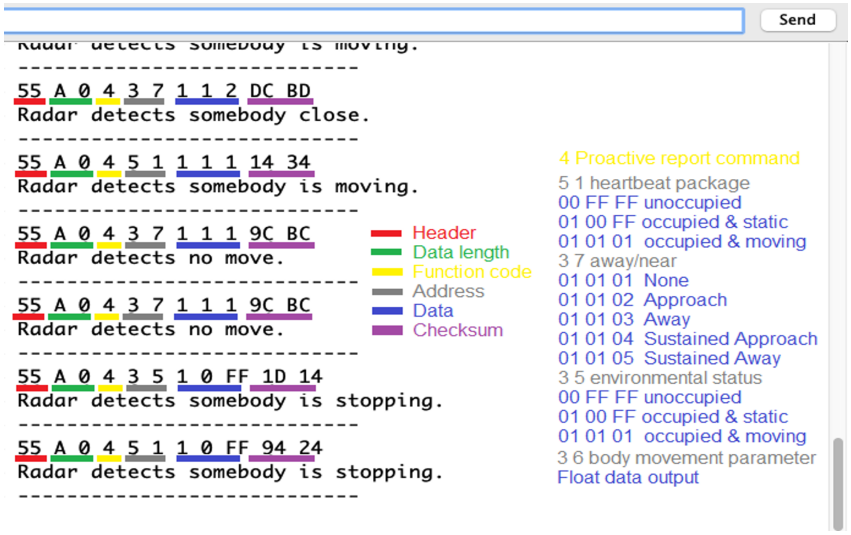



**Figure 4.5** Seeed Studio Human Detection Module output

5. **Seeed studio human detection lite module**: This sensor can detect small and micro motion through obstacles and it contain an advanced mode which give an output of raw data (more details will be explained in this chapter).

The 24GHz Lite Module was chosen for this project due to its ability to detect through wall and also ability to provide raw data, which is crucial for detailed analysis and model training.

**Table 4.1** Comparison of Sensors for Behind Wall Human Presence Detection

| **Sensor** | **Freq. (GHz)** | **Behind wall** | **Distance detection** | **Micro motion detection** | **Range (m)** | **Degree** | **Output** |
|---|---|---|---|---|---|---|---|
| **HB100 doppler** | 10.5 | No | No | Yes | 3 | ~ 90 | Raw data time series signal |
| **RCWL 0516** | 3.15 | wood | No | Slow motion, waving | 4.5–5 behind, 6 open area | 360 | Raw data time series signal |
| **Seeed Studio 24GHz lite module** | 24 | Non-metallic | yes | Yes | 4 - 5 | H 90, V 60 | Motion energies, distance |
| **Seeed Studio 24GHz module** | 24 | Non-metallic | No | Yes | ~3 behind, 12 open area | H 90, V 60 | Human parameter, human status |
| **Seeed Studio 24GHz sleep detection module** | 24 | No | No | Yes | 2.75 | H 40, V 40 | Human parameter, human status |

Human Static Presence Lite Module (MR24HPB1) [**69**][**70**] have been explored in order to detect human presence through walls. This radar module works with 24 GHz operating frequency with highly sensitive and immune to environmental interferences and applies FMCW ranging technology. The following are sensor specifications:

- Operating Voltage: 4.5 – 6 V
- Operating Current: 95 – 120 mA
- Operating Frequency: 24 GHz
- Detection Distance: 5 m
- Transmission Power: – 6.3 mW

The radar emits a 24 GHz millimeter-wave signal directed towards the detected object, which reflects this electromagnetic wave back to the radar unit. Within the radar system,

the transmitted signal undergoes decomposition, amplification, filtering, analog-to-digital conversion (ADC), and other signal processing stages to transform it into demodulated echo signal data. This data is subsequently transmitted to the microcontroller unit (MCU). Inside the MCU, the amplitude, frequency, and phase of these echo signals are analyzed to measure parameters such as respiration, movement, micro-movements, or to assess the environment [**69**][**70**]. Figure 4.6 illustrates the radar module, while Figure 4.7 depicts its operational principle.

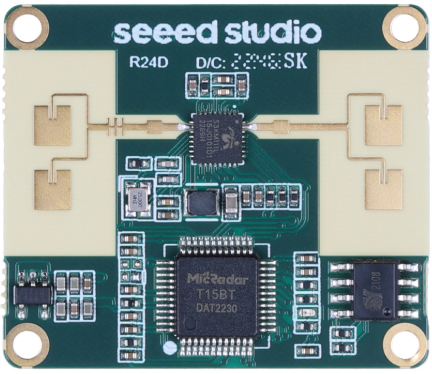



**Figure 4.6** mmWave FMCW Human Presence Module

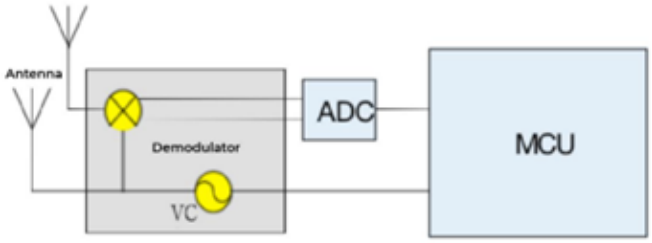



**Figure 4.7** Operating Principle

The optimal installation height for the radar ranges from 1 meter to 1.5 meters. It should be mounted horizontally, facing forward, and positioned at an angle no greater than ±5°. The radar can detect a moving human body (L3) within a range of up to 5 meters, detect a sitting or fidgeting human (L2) within a range of up to 4 meters, and detect the presence of a sleeping human (L1) within a range of up to 3 meters. Figure 4.8 illustrates the recommended installation configuration.

The mmWave radar module generates a time series output indicative of the presence or absence of humans. Sensor has 2 modes simple and advanced. In advanced mode the output is stationary energy, motion energy, distance for both and speed. In this experiment only motion energy was

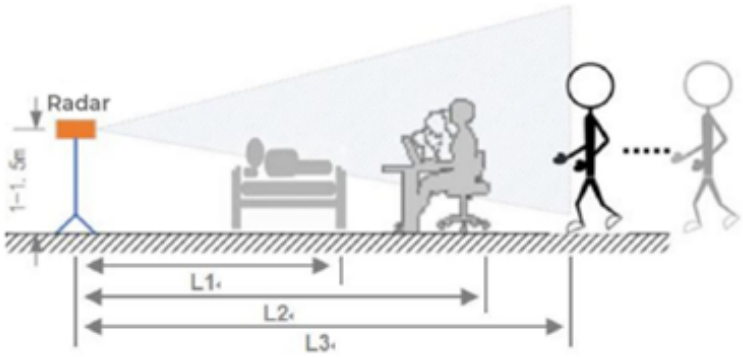



**Figure 4.8** Default Installation Setup

used as raw data. The motion energy value, ranging from 0 to 250, serves to offer feedback regarding the constant motion noise within an environment. In the absence of human presence, this value remains low, closely mirroring the ambient motion noise. However, with human motion detected, the motion energy value escalates, correlating directly with the intensity and proximity of the movement [**71**].

In our data collection setup, we utilized the Seeed Studio 24GHz mmWave Sensor - Human Static Presence Lite Module (MR24HPB1), interfaced with an Arduino microcontroller. The sensor communicates with the Arduino through the UART (Universal Asynchronous Receiver Rx/Transmitter Tx) serial port. To establish this connection, we connected the sensor's 5V pin to Arduino's 5V pin, GND to GND, RX to Arduino's soft serial TX pin, and TX to Arduino's soft serial RX pin, as outlined in the hardware diagram Figure 4.9. To avoid data confusion on the Arduino when using the Serial port for both output and data transmission, it is suggested to use a software serial port. The SoftwareSerial library needs to be imported, and the RX and TX pins (A2 and A3) defined in the program. This configuration enables seamless transmission of sensor data to the Arduino, where it is processed to detect and classify human presence and motion behind walls.

## 4.3 Data Collection Setups

The collected dataset encapsulates various conditions. Each entry in the dataset corresponds to a distinct instance of human presence, facilitating a nuanced analysis of movement patterns. Table 4.2 provides a comprehensive overview of the sensor setups used in this study, detailing the various conditions and configurations under which data was collected. Figure 4.10 provides a detailed overview of the data collection scenarios used in this study. The figure includes scenarios of a person remaining static, a person moving slowly, and a person moving quickly. The importance of capturing data with a person remaining static is underscored by the fact that, in some situations, individuals may be unable to move, possibly due to injury or entrapment

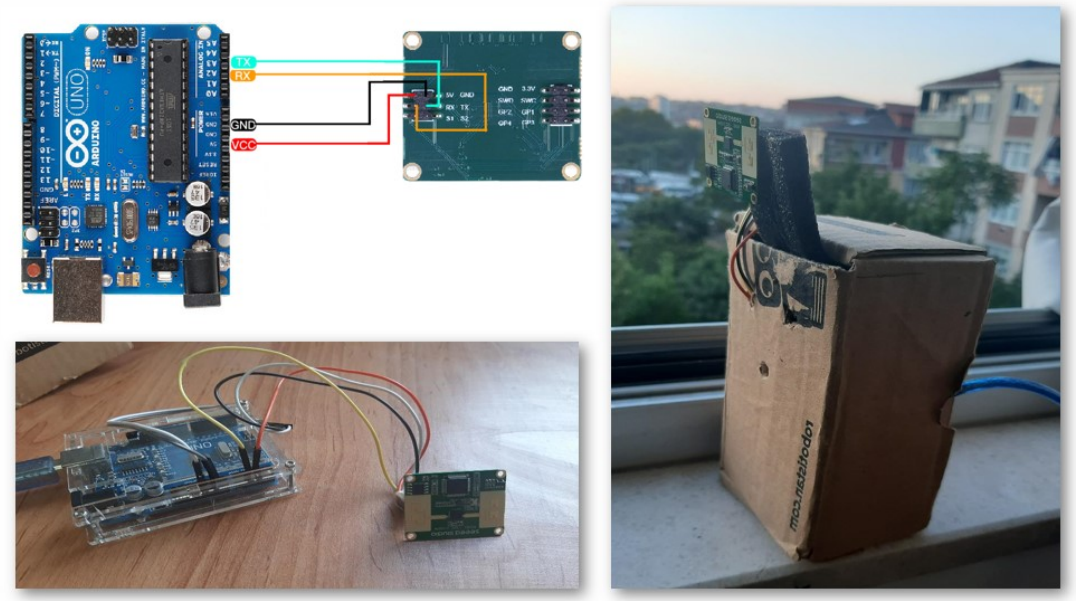



**Figure 4.9** Arduino/Sensor Interface.

under rubble. Slow movements are also critical as individuals trapped behind walls or under rubble may only be capable of making minimal motions, such as slight hand movements or subtle gestures. On the other hand, fast movements might indicate more vigorous activities, such as a person attempting to push away debris or making more noticeable efforts to signal for help. This comprehensive approach underscores the practical applications of the radar system in real-world disaster scenarios, where understanding the nature of human activity can significantly enhance rescue operations.

**Table 4.2** Measurement Setup

| **Condition** | **Variants** |
|---|---|
| **Person** | - No person<br>- Static<br>- Moving slowly<br>- Moving fast |
| **Obstacle's material** | - Wooden door $s \approx 4$ cm<br>- Wooden separator $s \approx 3$ cm<br>- Brick wall $s \approx 17$ cm |
| **Radar-obstacle distance** | $r = 5 - 10$ cm |
| **Obstacle-person distance** | - $d = 0$ m<br>- $d = 1$ m<br>- $d = 2$ m |

Dataset taken from 6 different volunteers, with different wall types and scenarios each one 2 – 5 minutes (Total $\approx$ 6 hours + 2 hours for out-of-sample testing data). Data was collected in a 5x5 meter room, utilizing a 4 cm thick wooden door as an obstacle. Additionally, measurements were taken behind a 17 cm thick wall. A further part of data collection occurred behind a 3 cm thick wooden separator

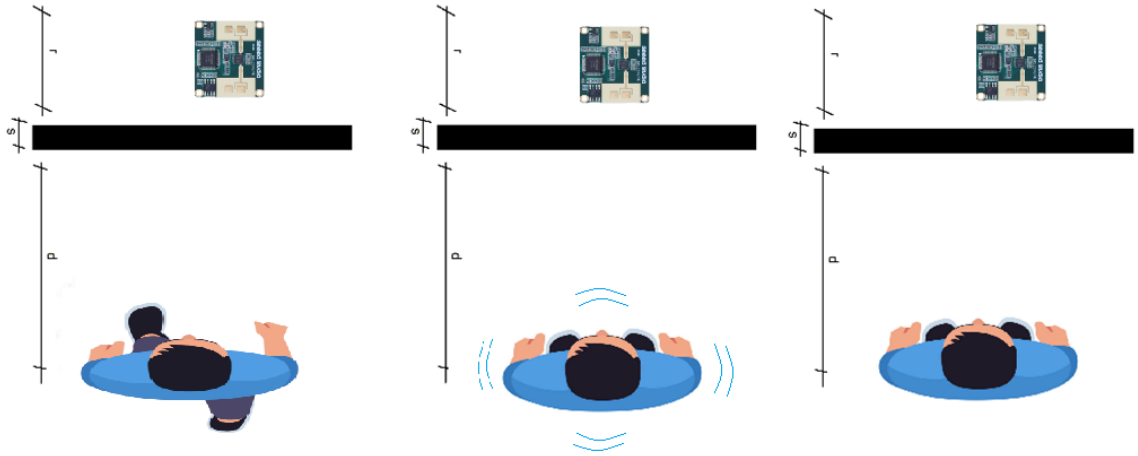


**Figure 4.10** Data Collection Scenarios a) Static, b) Slow Motion, c) Fast Motion.

in a classroom at the university with a total of 6 volunteers. In all data collection processes, sensor installation height was 1 meter.

Figure 4.11 shows the data collection environment.

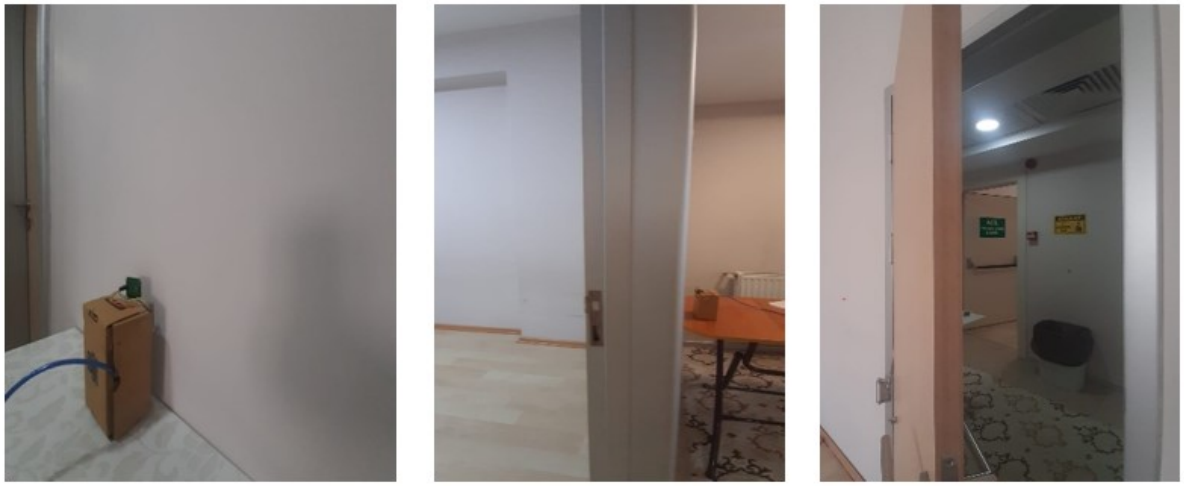


**Figure 4.11** Data Collection Environment a) Sensor Installation Behind Brick Wall, b) Brick Wall 17 cm Thickness, c) Wooden Door 4 cm Thickness.

### 4.3.1 Investigate FMCW Sensor for Action Recognition When No Barriers Exist

The sensor effectively detects various human actions when there are no barriers present. It can distinguish between different states such as motionless, active movement, and proximity (near/far). As shown in Figure 4.12, the provided output data indicates that the sensor reliably identifies when a person is moving or stationary, and whether they are close or distant.

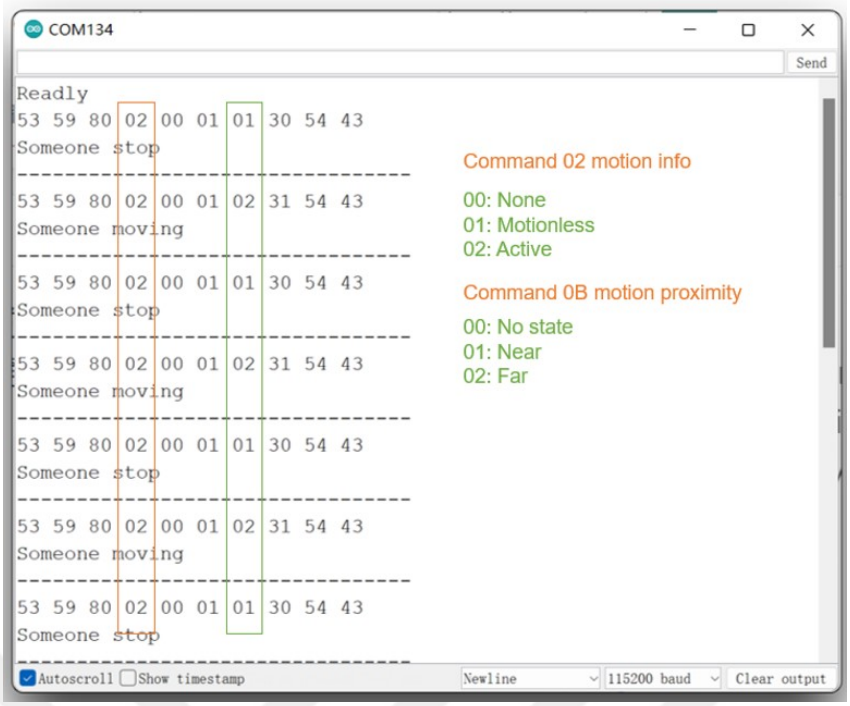



**Figure 4.12** Processed Output from Sensor When No Barriers Exist

The sensor operates in a simple mode and outputs processed data rather than raw data. However, in advanced mode employing motion energy values as raw data can enhance the sensor's ability to distinguish between different actions. Figures 4.13 and 4.14 represent different samples from a volunteer when no barrier exists for various motions. As shown, the peak frequency for fast motion is higher than for static and slow motion, demonstrating the sensor's capability to distinguish and test different actions.

The next step will involve these movements behind a wall. This will help assess the sensor's capability to accurately detect and classify human actions in more complex and obstructed environments.

### 4.3.2 Behind Wall Dataset

To understand how different wall materials affect the detection capabilities of the sensor different scenarios have been done under various conditions. Figure 4.15 illustrates detecting human presence and activity through different materials. It presents three distinct scenarios: no wall, a wooden wall, and a brick wall. X axis represents time points (seconds) while Y axis represents motion energy amplitude values. For each scenario, the sensor data is plotted to represent different human activities, including no one present, a person approaching the sensor, a person remaining static, and a person moving away from the sensor. The scinario can be explained as the person keep away from the sensor detedtion range (far than 5 meters) then start to approach near to the sensor until 1 meter or less then stop and just breath. After that the person go away until be out of range of detection of the sensor. It repeated three times with no wall, 4 cm wooden wall and 17 cm brick wall.This comparison highlights the sensor's ability to detect and differentiate human movements when obstacles like wood and brick are present. The variations in signal patterns between the different materials and activities are evident.

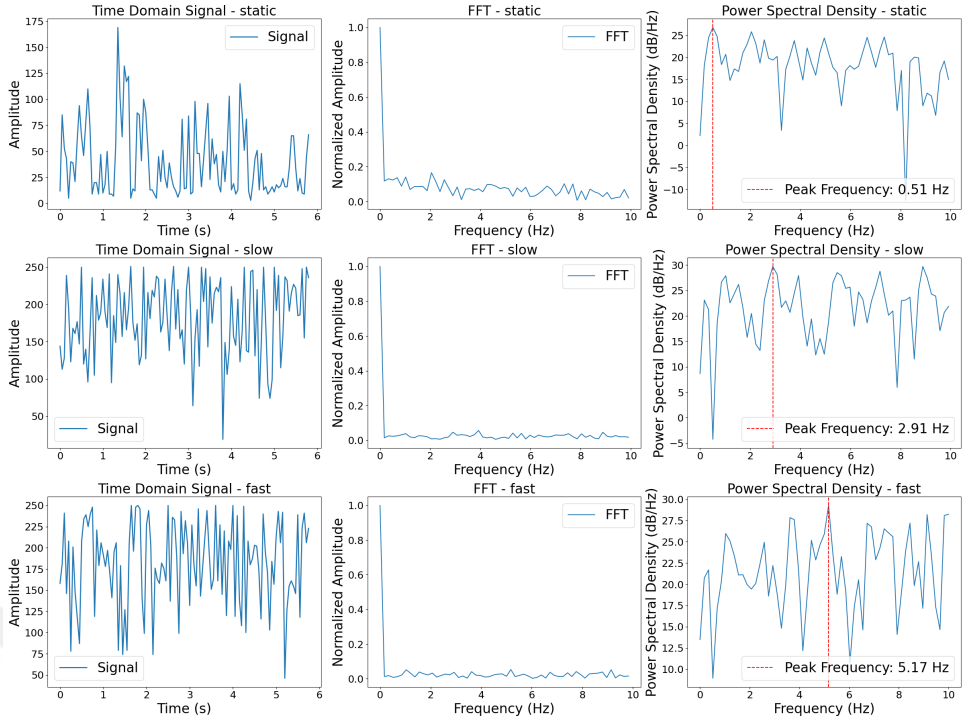



**Figure 4.13** Different Motion When No Barriers - Volunteer 1

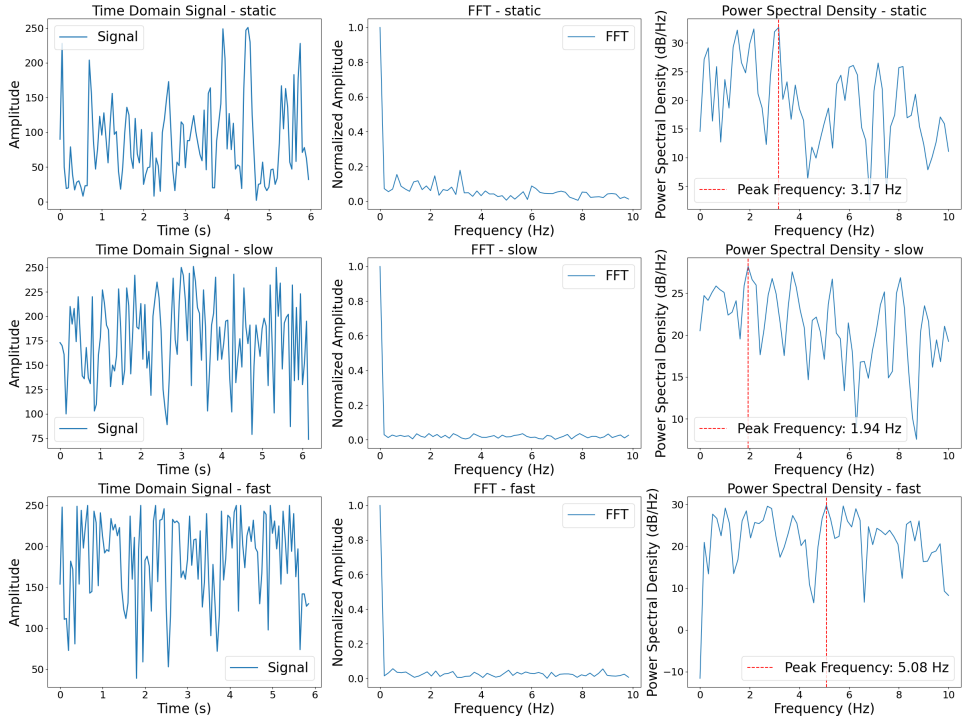



**Figure 4.14** Different Motion When No Barriers - Volunteer 2

- **Wall Type and Human Presence**

  Figures 4.16 and 4.17 illustrate the sensor readings for different wall types when there is no human presence and when a human is static behind the wall in time domain (time vs amplitude), frequency domain (frequency vs amplitude) and power spectrum density (PSD) (frequency vs

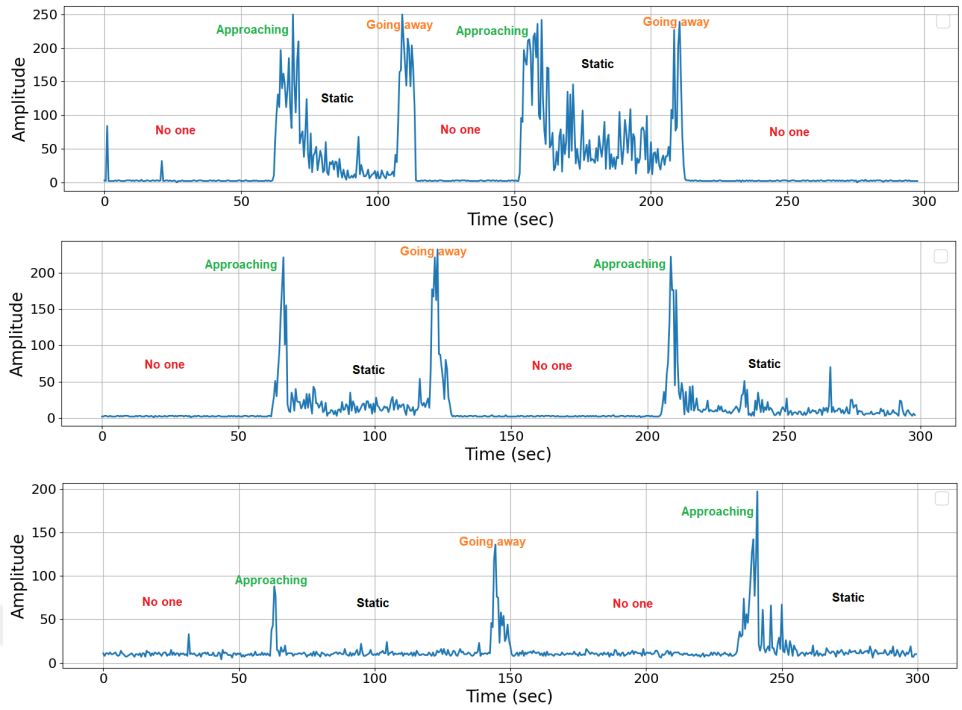



**Figure 4.15** Detecting Human Presence and Activity Through Different Materials; No wall, Wooden wall and Brick wall Respectively.

PSD value). These visualizations help in understanding the baseline readings of the sensors and how different wall materials affect the detection capability. When no one is present, the readings are relatively uniform, indicating minimal interference and PSD value below 0. In contrast, when a person is static behind the wall, slight variations in the readings can be observed in both time domain and different frequency amplitude values in frequency domain demonstrating the sensor's sensitivity to human presence even through various wall types.

- **Distance Behind the Wall** Figures 4.18 and 4.19 show the sensor readings for different distances behind different wall types in time domain (time vs amplitude), frequency domain (frequency vs amplitude) and power spectrum density (PSD) (frequency vs PSD value). As the distance between the wall and the human increases, the readings vary, indicating a diminishing detection signal with increasing distance.

- **Different Movements Behind the Wall**
  Figures 4.20 and 4.21 compare the sensor readings for different types of movements (static, slow motion, and fast motion) behind different wall types in time domain (time vs amplitude), frequency domain (frequency vs amplitude) and power spectrum density (PSD) (frequency vs PSD value). This visualization highlights how movement impacts the sensor readings, with faster movements generating more significant fluctuations in time domain while the power ranges became wider in power spectrum. Understanding these patterns is essential for distinguishing between different human activities and improving the model's accuracy in detecting and classifying human presence and movements.

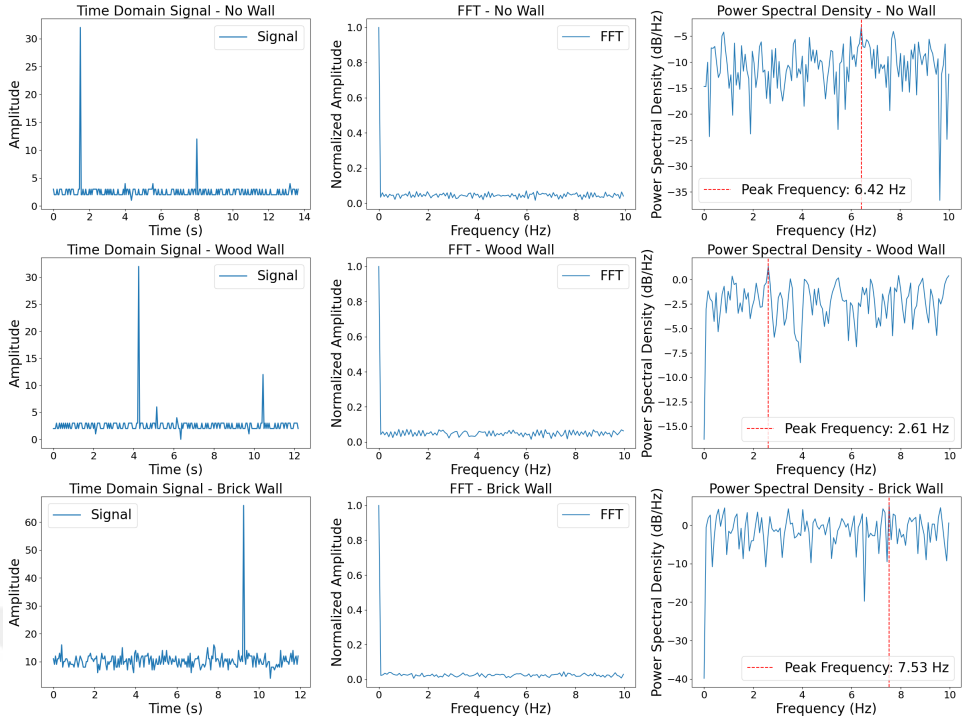



**Figure 4.16** Sensor Readings for Different Wall Types with No Human Presence.

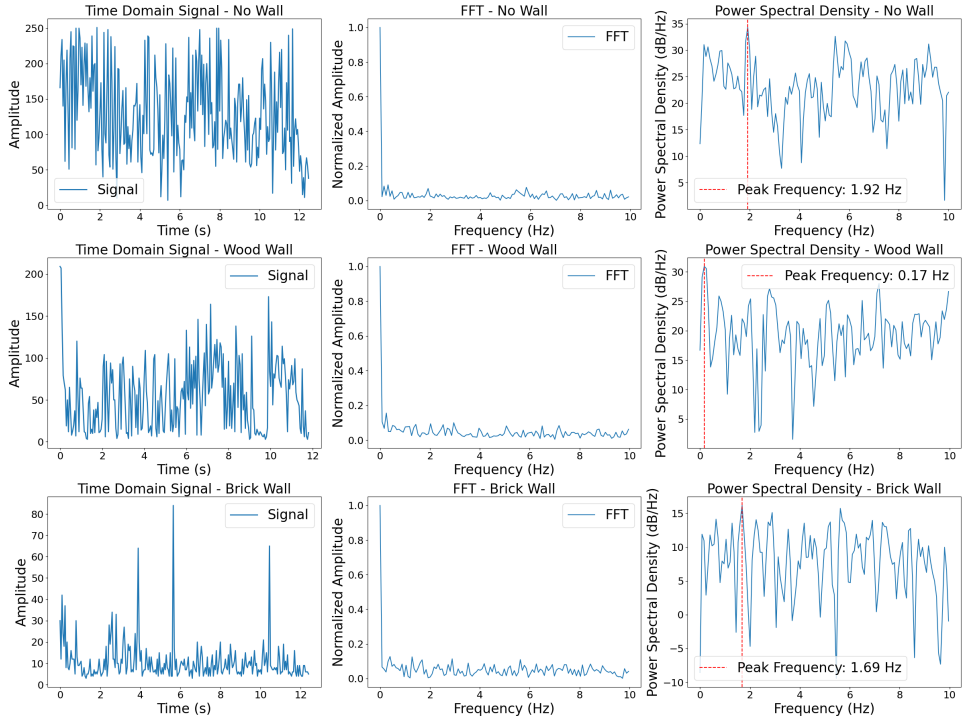



**Figure 4.17** Sensor Readings for Different Wall Types with Static Human.

- **Two people behind wall**

  Multiple samples were collected for the test involving two people positioned behind a wall. These samples included various scenarios: both individuals were static behind a wooden or brick barrier and one person was static while the other moved in place. Figure 4.22 provides a comparative

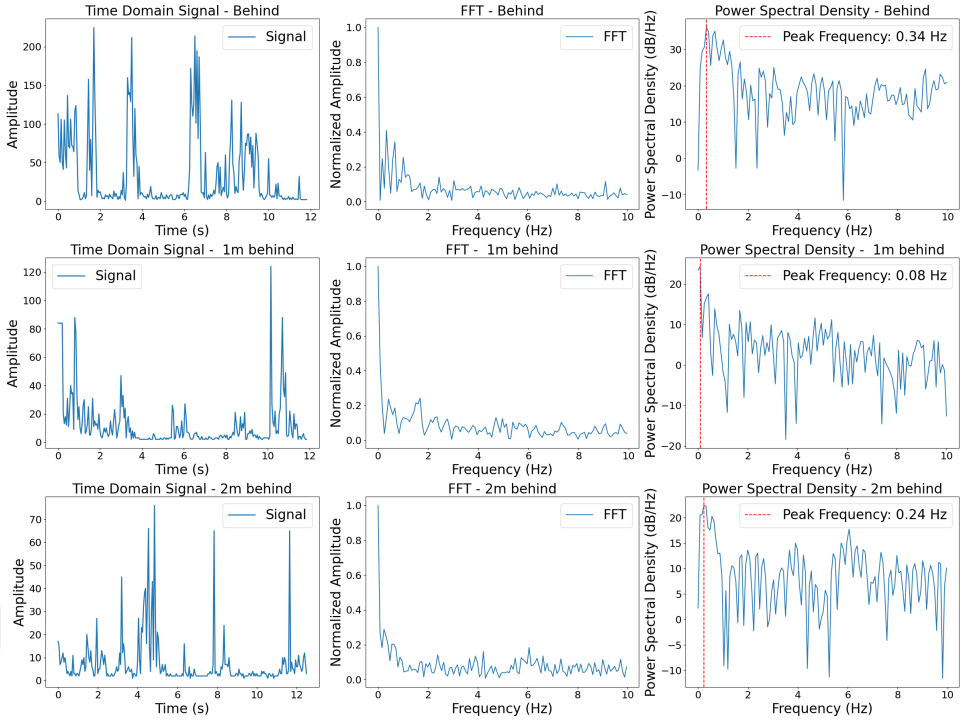



**Figure 4.18** Sensor Readings for Different Distances Behind 4cm Wooden Wall

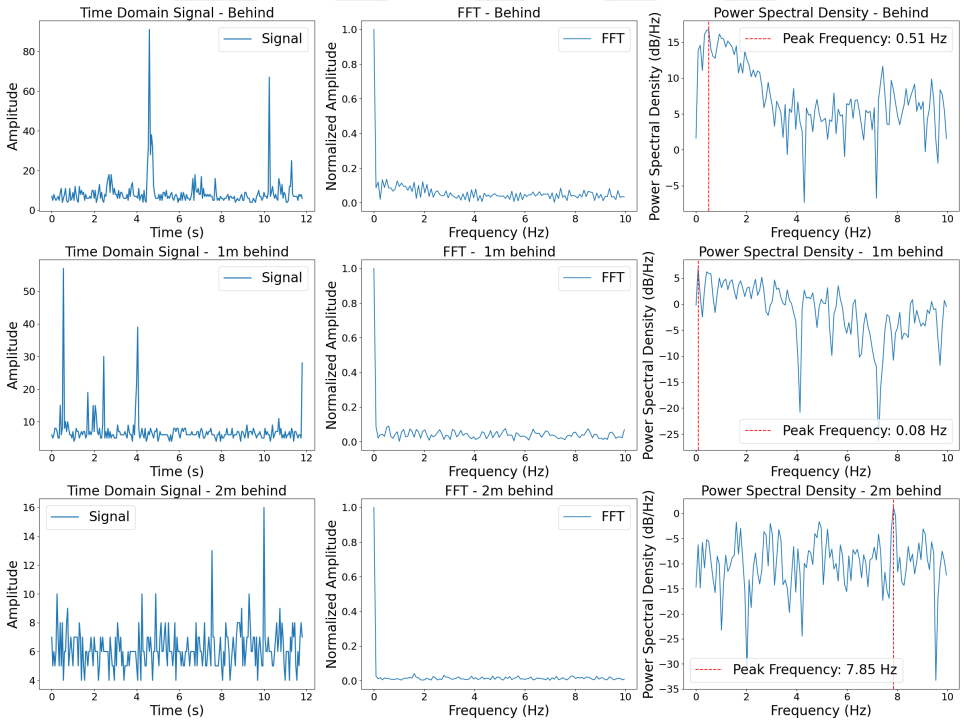



**Figure 4.19** Sensor Readings for Different Distances Behind 17 cm Brick Wall

analysis of the signal characteristics observed when one person was static versus when two people were either static or had one person moving.

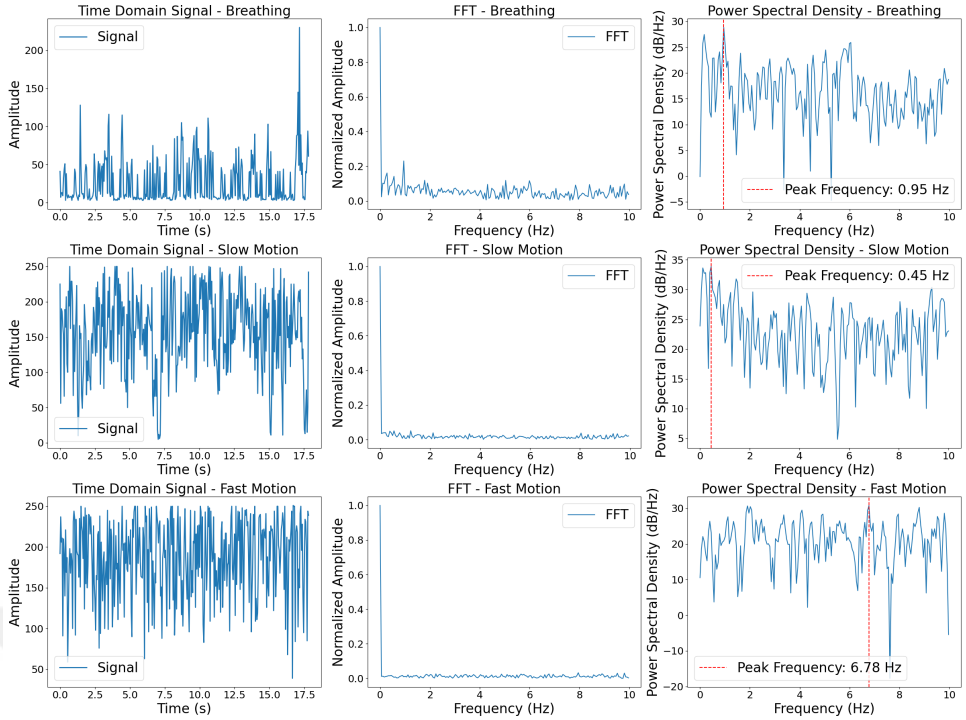



**Figure 4.20** Sensor Readings for Different Types of Movements Behind 4 cm Wooden Wall.

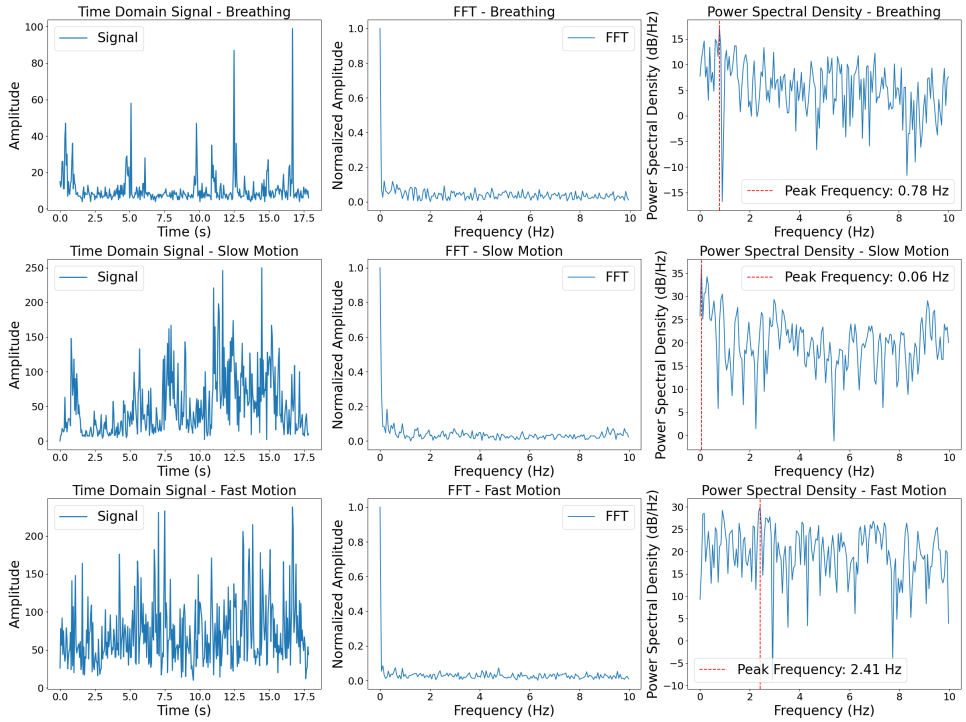



**Figure 4.21** Sensor Readings for Different Movements Behind 17 cm Brick Wall.

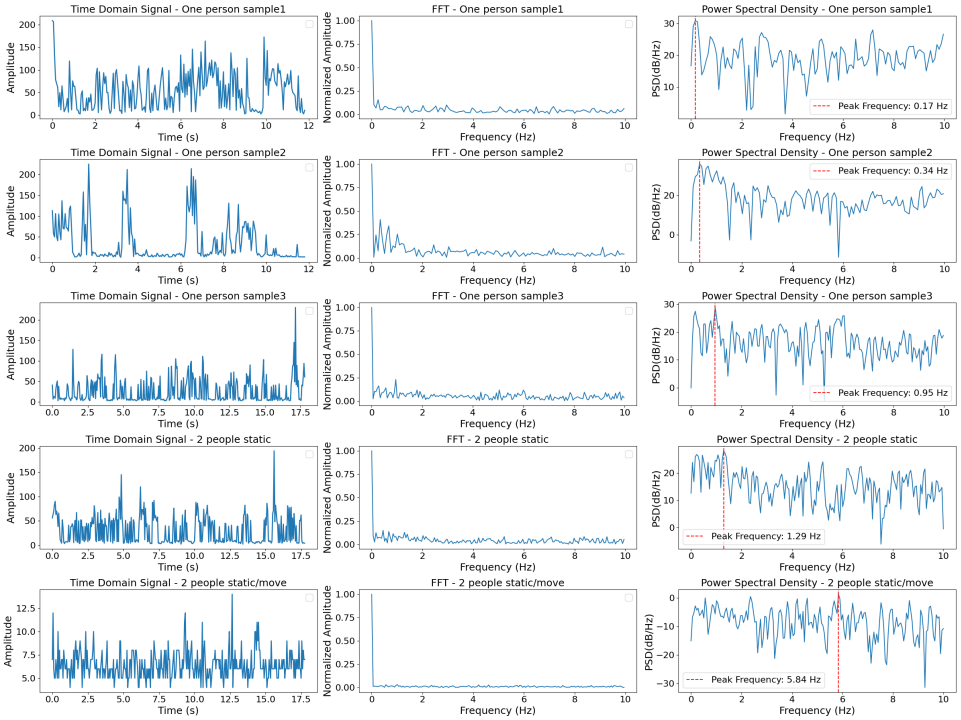



**Figure 4.22** Sensor Readings for Different Movements Behind 17 cm Brick Wall.

# 5
# RESULTS AND DISCUSSION

This section presents the results and discussion for human detection and action recognition using Frequency Modulated Continuous Wave (FMCW) radar for through-wall detection. The focus is on evaluating the impact of features selection on the accuracy of various machine learning models. The performance of different algorithms is compared based on datasets with varying numbers of features to identify the most effective approach for this application.

## 5.1 Through Wall Human Detection

This section introduces human detection process. After data is collected and processed, data is prepared for human detection models. Scaling, feature extraction and selection processes are explained below beside models' results.

### 5.1.1 Data Scaling

In this thesis, standard feature scaling techniques were evaluated after testing models across different scaling methods including standardization, min-max scaling and mean normalization scaling. Figure **??** shows the average accuracy for different scaling methods when applied to different models to raw time domain dataset, raw frequency domain dataset and features dataset. The standardization scaling method achieves the highest average score 87% exceeds min-max scaling by 1%.

### 5.1.2 Feature Extraction and Selection

The features extracted from the raw signal can be broadly categorized into time domain, and frequency domain features as explained in chapter 3. To address feature selection and the effect of feature numbers on the human detection models, table 5.1 represents a detailed ranking of features. In this study, feature importance was calculated using three different methods: Random Forest (RF), Recursive Feature Elimination (RFE), and Mutual Information (MI). For each feature, RF and MI directly provided importance scores, while RFE provided ranks, which were inverted to obtain importance scores ($\frac{1}{\text{rank}}$). These importance scores were then combined by averaging them to get a unified importance score for each feature. The final rank of each feature was determined by sorting these combined importance scores in

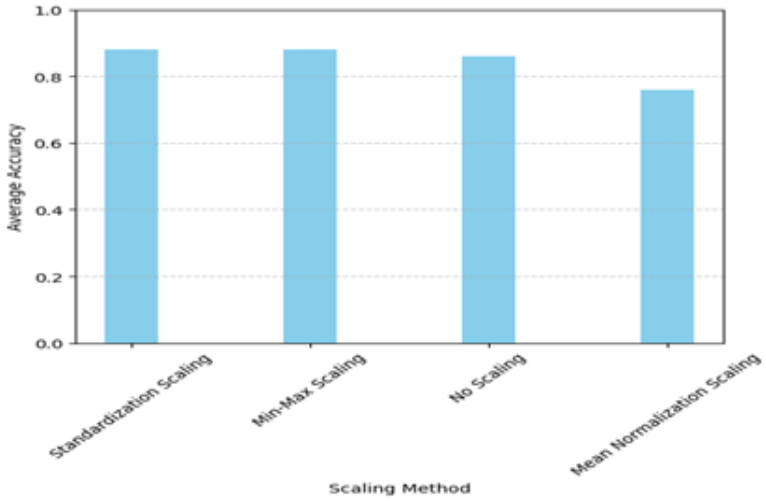



**Figure 5.1** Average Performance of Scaling Methods Across Datasets.

descending order. Specifically, if $\text{RF}_i$, $\text{RFE}_i$, and $\text{MI}_i$ are the importance scores for the $i$-th feature from RF, RFE, and MI respectively, the combined importance score $C_i$ is calculated as:

$$C_i = \frac{\text{RF}_i + \text{RFE}_i + \text{MI}_i}{3} \tag{5.1}$$

Features were then ranked based on these combined scores, ensuring consistent and robust feature selection. The top features identified in the analysis include Total Power, Power, and Energy, which demonstrate significant importance across multiple ranking methods. These features offer a comprehensive view of the signal's characteristics, capturing various aspects of power, variability, and complexity. Top 7 features are listed below.

- Total Power ranked the highest, it measures the aggregate power over the signal's duration.
- The power feature measures the signal's instantaneous power, detailing variations in strength over time.
- Energy quantifies the overall power within a signal, indicating its intensity and stability. Its high ranking reflects its comprehensive representation of the signal's characteristics. Combined with Power and Total Power, it captures different aspects of the signal's power distribution.
- RMS provides an effective measure of the signal's magnitude, reflecting its variability and stability.
- Mean represents the average value of the signal, summarizing its overall behavior. Its high ranking shows its effectiveness in complementing the information provided by Energy and Total Power.
- Entropy measures the signal's complexity and disorder, providing insights into the unpredictability and information content of the signal.

- Standard Deviation important for measuring signal variability, combined with Mean's central tendency, helps understand the signal's overall behavior.

**Table 5.1** Sorted Combined Feature Importance

| Feature | Combined Importance |
|---|---|
| **Total_Power** | 0.528560 |
| **Power** | 0.519627 |
| **Energy** | 0.519546 |
| **RMS** | 0.512870 |
| **Mean** | 0.507400 |
| **Entropy** | 0.498695 |
| **Std.deviation** | 0.495743 |
| **SD/mean ratio** | 0.449003 |
| **Skewness** | 0.386528 |
| **Mobility** | 0.381333 |
| **Variance** | 0.327102 |
| **SHANNON_Entropy** | 0.232653 |
| **Form Factor** | 0.200300 |
| **Median** | 0.189824 |
| **Max - min squared** | 0.187589 |
| **xMax** | 0.185478 |
| **Max - min** | 0.180653 |
| **Max/min ratio** | 0.143326 |
| **FKurtosis** | 0.140470 |
| **FVariance** | 0.136996 |
| **Kurtosis** | 0.097802 |
| **xmin** | 0.091512 |
| **Mean_Frequency** | 0.057250 |
| **FSkewness** | 0.049540 |
| **Turns Count** | 0.037126 |
| **median_frequency** | 0.029016 |
| **Correlation** | 0.021085 |

### 5.1.3 Human Detection Models

In the process of applying human detection models to the dataset, several critical steps are undertaken to ensure optimal performance. Initially, various machine learning models are defined along with their respective hyperparameter grids for tuning. These models include Support Vector Machine (SVM), K-Nearest Neighbors (KNN), Decision Tree (DT), Naive Bayes (NB), Logistic Regression (LR), and Random Forest (RF). Each model's performance is rigorously evaluated using 5-fold cross-validation, which splits the training data into five parts, training on four and validating on one, iterating this process five times. This method reduces variance and provides a more reliable performance estimate. Hyperparameter tuning is performed via grid search, systematically testing combinations of hyperparameters to identify the best-performing parameters for each model. After training, the best parameters are selected based on the highest accuracy, and models are evaluated using confusion matrices and classification reports to provide detailed performance metrics. This comprehensive evaluation facilitates the selection of the most suitable model with optimal hyperparameters for the dataset. Table 5.2 shows the hyperparameters used for each model.

**Table 5.2** Hyperparameters for Each Model

| Model | Hyperparameters |
|---|---|
| **SVM** | {'kernel': ['linear', 'poly', 'rbf', 'sigmoid']} |
| **KNN** | {'n_neighbors': [3, 5, 7]} |
| **DT** | {'max_depth': [None, 10, 20, 30]} |
| **NB** | {} (Default: priors=None, var_smoothing=1e-9) |
| **LR** | {'C': [0.1, 1, 10]} |
| **RF** | {'n_estimators': [10, 50, 100]} |

Different datasets and their performance with various machine learning algorithms have been examined, the choice of dataset plays a crucial role in achieving optimal results. Figure 5.2 shows different models applied to raw time domain, raw FFT and features datasets.

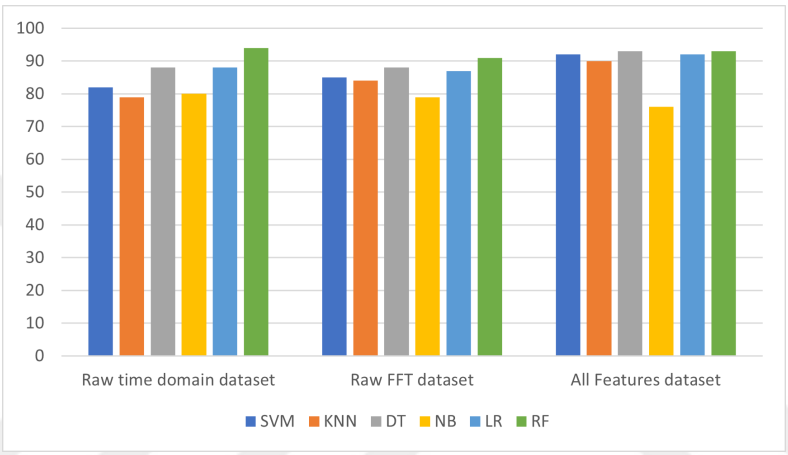



**Figure 5.2** Evaluation Accuracy of Different Models with Different Datasets.

- Raw time domain dataset: The accuracies range from 79% (KNN) to 94% (RF). This dataset provides moderate performance with RF achieving the highest accuracy. Other notable accuracies include SVM at 82%, DT at 87%, NB at 80%, and LR at 88%.
- Raw FFT dataset: The accuracies range from 79% (NB) to 90% (RF). This dataset performs reasonably well, with SVM and KNN showing similar performance at 85% and 84%, respectively, compared to the time domain dataset. However, there are slight improvements for DT and LR over the time domain dataset, indicating that frequency domain information can be valuable for these models. Specifically, DT reaches 88%, and LR is at 87%.
- All features dataset: This dataset yields the highest accuracies, ranging from 76% (NB) to 94% (RF). Notably, every algorithm performs better or equally well on this dataset compared to the other two datasets, highlighting the effectiveness of the feature extraction process. SVM achieves 92%, KNN reaches 90%, DT achieves 92%, and LR is at 92%.

The all-features data set stands out as the best among the three, demonstrating significant improvements in accuracy for all algorithms. Raw data, whether in the time domain or frequency domain, contains a

wealth of information, but it also includes noise and irrelevant details that can hinder model performance. By selecting and extracting relevant features, the most significant information will be extracted, making it easier for the algorithms to learn and generalize from the data.

### 5.1.4 The Effect of Feature Selection on System Performance

Figure 5.3 shows the classification accuracies of different machine learning algorithms (Support Vector Machine (SVM), K-Nearest Neighbors (KNN), Decision Tree (DT), Naive Bayes (NB), Logistic Regression (LR)) with varying numbers of selected features: 5, 10, 15, 20, and all features.

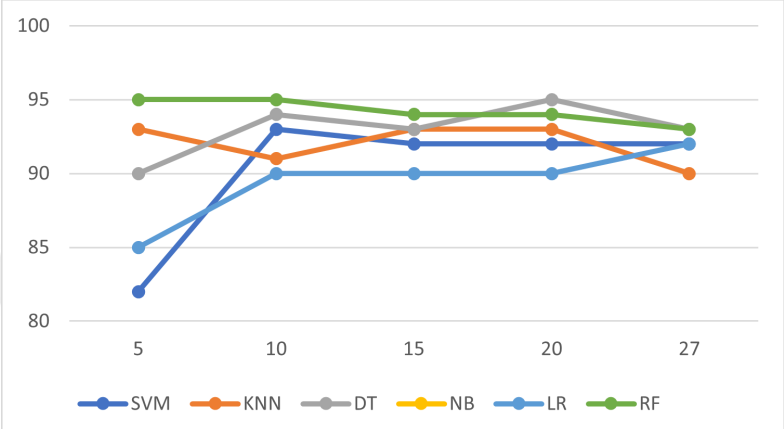



**Figure 5.3** Accuracy Vs Feature Number for Binary Classification

- With 5 features: Random Forest (RF) achieved the highest accuracy at 95%, followed closely by KNN at 93%, Decision Tree (DT) at 90%, Logistic Regression (LR) at 85%, SVM at 82%, and Naive Bayes (NB) at 75%. This indicates that with a smaller feature set, RF is the most effective in capturing relevant patterns in the data.

- With 10 features: RF and DT both showed the highest accuracy at 95% and 94%, followed by SVM at 92%, KNN at 91%, Logistic Regression (LR) at 90%, and NB at 77%. The increase in the number of features led to improved performance for RF and DT, suggesting these algorithms benefit from additional information.

- With 15 features: RF maintained an accuracy of 94%, DT and KNN both achieved 93%, while SVM also had an accuracy of 92%. Logistic Regression (LR) scored 90%, and NB remained at 76%. This indicates that RF, DT, and KNN continue to perform robustly with more features, while SVM and LR also benefit from the added features.

- With 20 features: Decision Tree (DT) achieved the highest accuracy at 95%, matched by KNN, while Random Forest (RF) showed 94% accuracy. SVM maintained 92%, Logistic Regression (LR) also had 90%, and Naive Bayes (NB) remained at 76%. This consistency suggests that DT, KNN, and RF are particularly robust to changes in feature number, while other algorithms show stable performance.

- With all features (27): SVM and Logistic Regression (LR) both achieved an accuracy of 92%, followed by Random Forest (RF) at 93%, Decision Tree (DT) at 93%, KNN at 90%, and Naive Bayes (NB) at 76%. This indicates that RF, DT, and LR continue to perform well with a large feature set, while KNN and SVM also show high accuracy.

Overall, the number of features selected significantly impacts the performance of the classifiers. Random Forest achieves optimal performance with 5 features, while Decision Tree performs best with 20 features. KNN performs consistently well with any number of features, SVM benefits from more features, and Naive Bayes remains stable regardless of feature count. These findings highlight the importance of selecting an appropriate number of features tailored to the specific algorithm to achieve the best classification performance. Table 5.3 shows the classification reports for human detection models when trained by 10 features.

**Table 5.3** Classification Report for Human Detection on 10 Features Dataset

| **Metric/Model** | | **SVM** | **KNN** | **DT** | **NB** | **LR** | **RF** |
|---|---|---|---|---|---|---|---|
| **Accuracy** | | 92 | 91 | 94 | 77 | 90 | 95 |
| **Precision** | **No Human** | 84 | 79 | 90 | 60 | 81 | 90 |
| | **Human** | 97 | 100 | 96 | 98 | 96 | 97 |
| **Recall** | **No Human** | 91 | 100 | 92 | 97 | 92 | 95 |
| | **Human** | 95 | 86 | 95 | 66 | 89 | 95 |
| **F1-score** | **No Human** | 94 | 88 | 91 | 74 | 86 | 92 |
| | **Human** | 89 | 93 | 95 | 79 | 92 | 96 |

*SVM(rbf), KNN(k=7), DT (max_depth= 20), LR (c=10), RF (n_estimator= 10)

Figure 5.4 shows confusion matrix for all model applied on 10-features dataset. The training dataset consists of a total of 444 instances, with 170 instances classified as Class 0 indicating no human presence, and 274 instances classified as Class 1 indicating human presence. The test dataset comprises 112 samples, divided into 38 samples labeled with Class 0 (no human presence) and 74 samples labeled with Class 1 (human presence).

These matrices reveal the number of true positives, false positives, true negatives, and false negatives, providing insights into each model's accuracy and error distribution. For instance, the SVM model shows perfect true negatives with 38 correctly identified negatives and high true positives with 66, but it has 8 false negatives. KNN also has 38 true negatives but slightly more false negatives at 10. DT performs well with 35 true negatives and 70 true positives, though it has 3 false positives. NB, however, has the highest number of false negatives (25) and shows less reliable performance compared to other models. LR exhibits consistent performance with 35 true negatives and 66 true positives, similar to SVM but with a few more false negatives. RF demonstrates strong performance with 36 true negatives and 70 true positives, having a balanced distribution of true positives and true negatives, and only 2 false positives. These observations from the confusion matrices underscore the varying capabilities of each model in handling binary classification tasks, highlighting their strengths and areas for improvement. Figure 5.5 shows the ROC-AUC curve for all models.

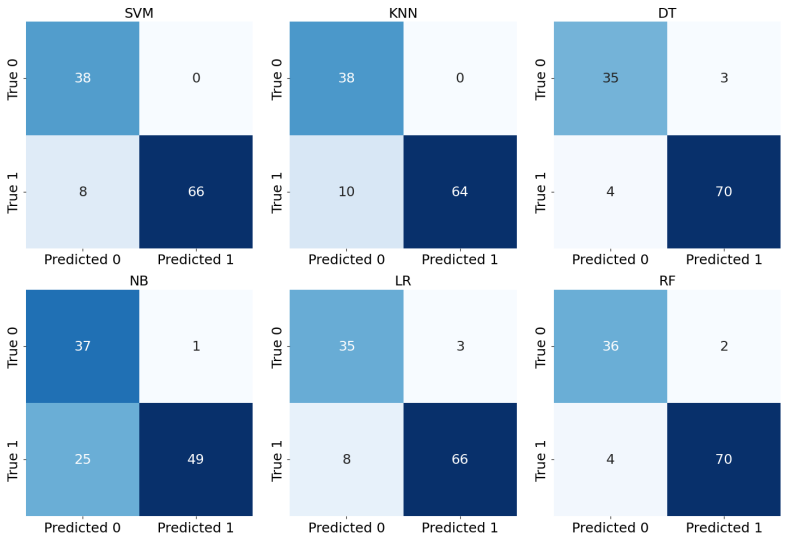



**Figure 5.4** Confusion Matrix for All Models with Features Dataset.

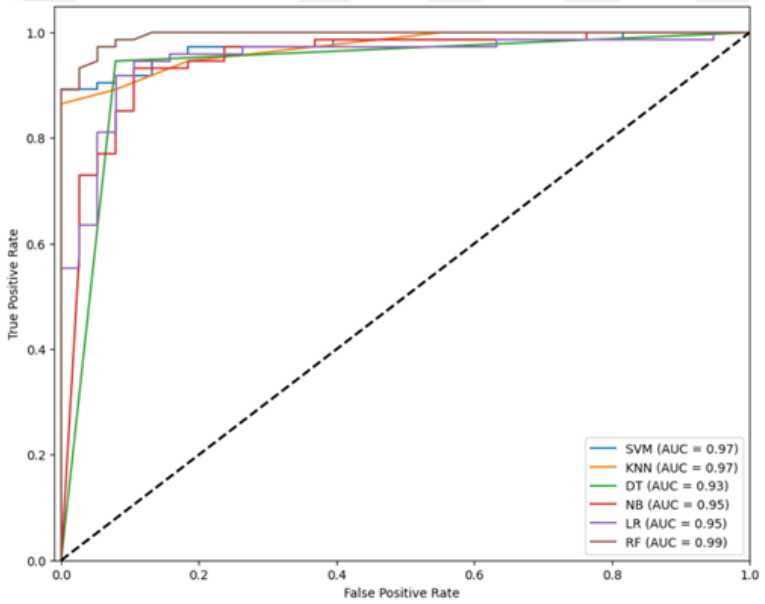



**Figure 5.5** ROC-AUC for All Models (with 10 Features Trained Model)

## 5.2 Through Wall Action Recognition

The initial binary classification showed good performance with 95% using RF model, demonstrating the effectiveness of the machine learning algorithms on simpler tasks. To extend this capability to more complex scenarios, a modification was made to adapt the models for multi-class classification. This adaptation allows the system to recognize and categorize different types of human actions through a wall. The new classification scheme includes four classes: (static, slow movement, and fast movement). The performance of various machine learning algorithms was evaluated on through-wall dataset expanded from binary to three classes, and similar to previous steps it tested in three formats: raw time domain, raw FFT, and a features dataset. Algorithms included SVM, KNN, DT, NB, LR, and RF. From figure 5.6 we can conclude that,

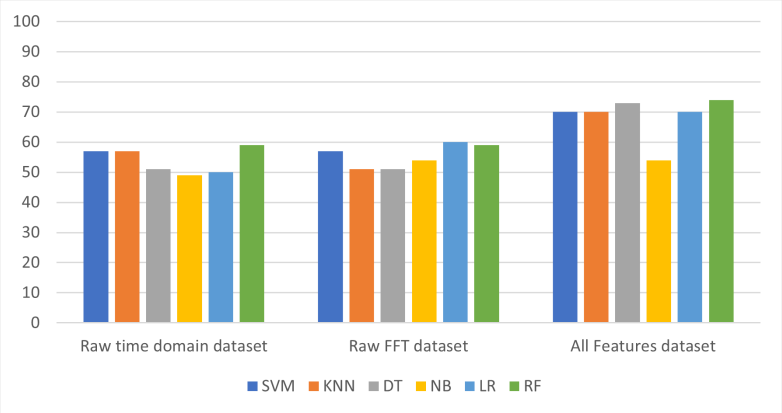



**Figure 5.6** Evaluation Accuracy of Different Models with Different Datasets (Action Recognition).

- Raw time domain dataset: Accuracies ranged from 52% (NB) to 62% (RF). This dataset shows moderate performance, with RF achieving the highest accuracy, followed by SVM at 57%, KNN at 55%, DT at 58%, and LR at 54%.
- Raw FFT dataset: Accuracies ranged from 49% (NB) to 62% (DT). This indicates that frequency domain information provides some improvement for DT, while other algorithms show moderate performance: RF at 60%, KNN at 59%, SVM at 54%, and LR at 55%.
- Features dataset: This dataset yielded the highest accuracies, ranging from 50% (NB) to 78% (RF), with all algorithms performing better than on the raw datasets. Specifically, SVM achieved 73%, KNN 70%, DT 69%, and LR 71%.

### 5.2.1 Initial Three Classes Classification

The initial approach involved classifying actions into three categories: static, slow movement, and fast movement. Feature selection process has been applied to features dataset. Figure 5.7 illustrates the classification accuracies of various machine learning algorithms across different numbers of selected features (see appendix A for selected features).

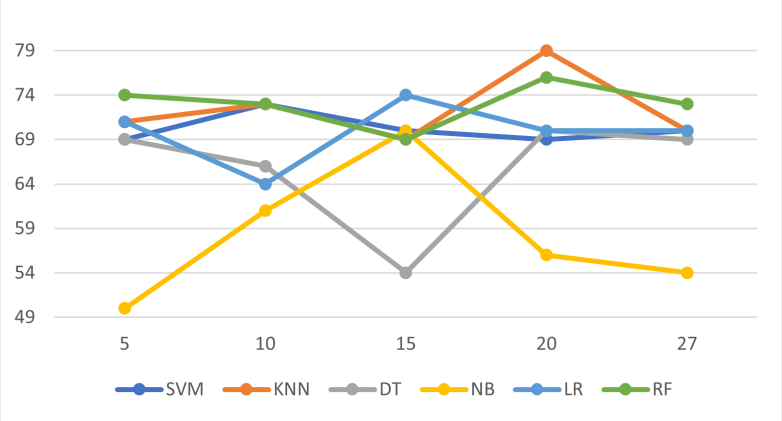



**Figure 5.7** Accuracy Vs Feature Number for Action Recognition.

As the number of features increases from 5 to 27, most algorithms show varying performance trends, particularly in KNN, DT, and RF. SVM starts at 69% accuracy with 5 features and remains consistent, ending at 70% accuracy with all features. KNN starts at 71% with 5 features, peaks at 79% with 20 features, and slightly decreases to 70% with all features. DT starts at 69% with 5 features, dips to 54% with 15 features, then improves to 70% with 20 features and 69% with all features. NB shows the lowest performance, ranging from 50% to 70%, indicating its limitations in capturing nuanced patterns. LR shows stable performance, starting at 71% with 5 features and remaining around 70% with more features. RF performs the best overall, with accuracies ranging from 74% to 76%, demonstrating robustness in handling varying feature complexity. Overall, these results underscore the importance of feature selection in optimizing model performance. SVM and LR are less sensitive to changes in the number of features, while RF, KNN, and DT show potential for improved accuracy with optimal feature selection. Naive Bayes remains consistently lower, highlighting its relative limitations. Table 5.4 shows more details about classification reports for all models when applied into 20 features dataset for action recognition. Figure 5.8 shows confusion matrix for all model applied on feature dataset for the 3 classes,

**Table 5.4** Classification Report for Action Recognition on Features Dataset

| **Metric/Model** | | **SVM (RBF)** | **KNN** | **DT** | **NB** | **LR** | **RF** |
|---|---|---|---|---|---|---|---|
| **Accuracy** | | 69 | 79 | 70 | 56 | 70 | 76 |
| **Precision** | **Static** | 77 | 80 | 83 | 60 | 76 | 79 |
| | **Fast** | 80 | 87 | 63 | 46 | 69 | 80 |
| | **Slow** | 50 | 70 | 59 | 44 | 62 | 68 |
| **Recall** | **Static** | 80 | 93 | 80 | 97 | 83 | 87 |
| | **Fast** | 67 | 72 | 67 | 33 | 61 | 67 |
| | **Slow** | 55 | 64 | 59 | 18 | 59 | 68 |
| **F1-score** | **Static** | 79 | 86 | 81 | 74 | 79 | 83 |
| | **Fast** | 73 | 79 | 65 | 39 | 65 | 73 |
| | **Slow** | 52 | 67 | 59 | 26 | 60 | 68 |

*SVM(linear), KNN(k=7), DT (max_depth= 20), LR (c=0.1), RF (n_estimator= 100)

the movement types in the dataset are represented by the following: 0 for ‘static, 1 for ’human moving fast’, and 2 for ’human moving slow’. In the training dataset, there are a total of 278 instances distributed across three classes (95 sample static, 80 sample human moving fast and 103 sample for human moving slow). Test data contains 70 samples; 30 sample static,18 sample human moving fast and 22 sample humans moving slow).

The SVM model shows a good detection rate for the first class with 27 true positives but struggles with the second and third classes, reflected in the higher number of misclassifications. KNN exhibits a strong performance across all classes, with fewer misclassifications, particularly for the second class. DT shows moderate performance, with some misclassifications across all classes. NB, while having the highest true positives for the first class, significantly misclassifies the second and third classes, indicating its limitations. LR performs consistently but has a few misclassifications, particularly in the second class. RF demonstrates robust performance with a balanced distribution of true positives and fewer misclassifications across all classes. These observations from the confusion matrices highlight the varying strengths and weaknesses of each model in handling multi-class classification tasks.

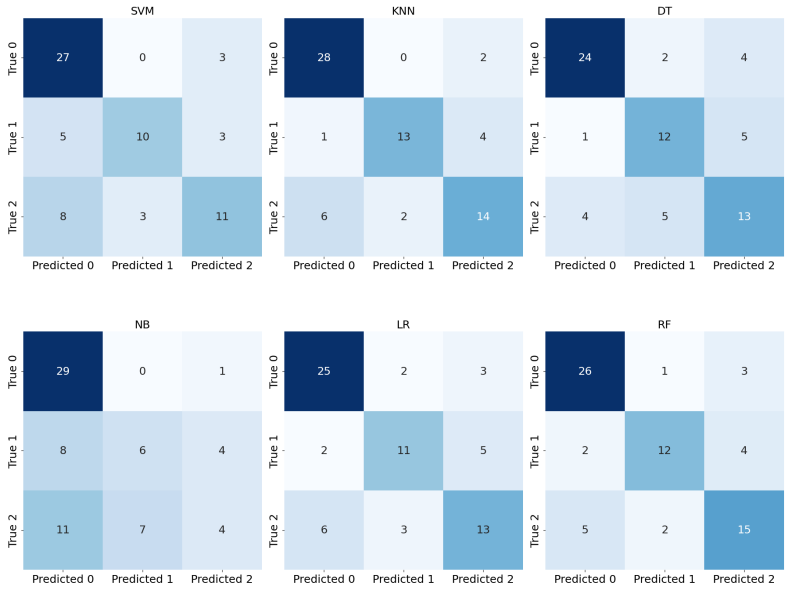



**Figure 5.8** Confusion Matrices for Action Recognition.

### 5.2.2 Merging Classes into Static and Movement

Due to the challenges faced with the three-class classification, the slow and fast movement classes were merged into a single "movement" class, resulting in a binary classification problem with the classes being static and movement. Table 5.5 presents the classification report for action recognition using a dataset with 20 features. This table compares the performance of six different machine learning models: SVM, KNN, DT, NB, LR, and RF. The metrics evaluated include accuracy, precision, recall, and F1-score for two classes: "Static" and "Movement."

**Table 5.5** Classification Report for Binary Action Recognition.

| **Metric/Model** | | **SVM (RBF)** | **KNN** | **DT** | **NB** | **LR** | **RF** |
|---|---|---|---|---|---|---|---|
| **Accuracy** | | 81 | 81 | 84 | 71 | 79 | 90 |
| **Precision** | **Static** | 84 | 81 | 83 | 60 | 83 | 87 |
| | **Movement** | 80 | 81 | 85 | 95 | 77 | 92 |
| **Recall** | **Static** | 70 | 73 | 80 | 97 | 63 | 90 |
| | **Movement** | 90 | 88 | 88 | 53 | 90 | 90 |
| **F1-score** | **Static** | 76 | 77 | 81 | 74 | 72 | 89 |
| | **Movement** | 85 | 84 | 86 | 68 | 83 | 91 |

*SVM(rbf), KNN(k=7), LR (c=50), RF (n_estimator= 10)

The accuracy scores highlight that RF achieves the highest accuracy at 90%, followed by DT at 84%, SVM and KNN both at 81%, LR at 79%, and NB at 71%. Precision, recall, and F1-score metrics provide a detailed view of each model's ability to correctly identify "Static" and "Movement" actions. For instance, RF demonstrates superior precision for "Movement" (92%) and strong recall for both static and movement (90%), leading to high F1-scores for both actions. Conversely, NB shows lower performance metrics across the board, particularly in precision for "Static" (60%) and recall for "Movement" (53%). This detailed classification report underscores the strengths and weaknesses of each model, providing insights into their effectiveness in action recognition tasks with a 20-feature dataset. Figure 5.9 shows

confusion matrix for all model applied on feature dataset for the 3 classes, the movement types in the dataset are represented by the following: 0 for ‘static, 1 for ’movement’.

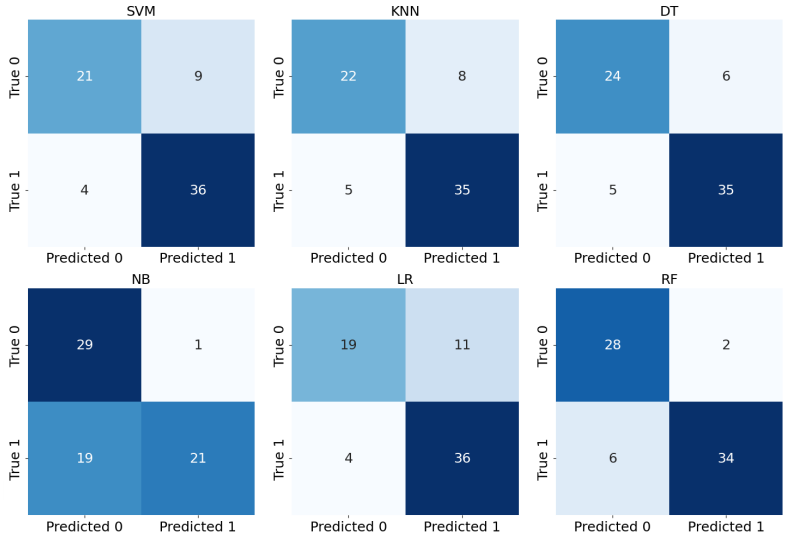



**Figure 5.9** Confusion Matrix for Static/Movement Action Recognition.

To analyze the performance of the models in classifying "Static" and "Movement" actions, we examined the confusion matrices for each algorithm. These matrices provide a clear breakdown of true positives, false positives, true negatives, and false negatives. For instance, the SVM model shows 21 true negatives and 36 true positives, with 9 false positives and 4 false negatives. KNN is similar, with 22 true negatives and 35 true positives. DT performs slightly better with 24 true negatives and 35 true positives. NB has a high number of true negatives (29) but also the highest number of false negatives (19), indicating a struggle with detecting "Movement" actions. LR shows 19 true negatives and 36 true positives, with a relatively higher number of false positives (11). RF demonstrates strong performance with 28 true negatives and 34 true positives, and low false positives (2). These observations highlight the strengths and limitations of each model in distinguishing between "Static" and "Movement" actions, with RF and DT showing particularly robust performance.

## 5.3 Out-of-Sample Testing

Out-of-sample testing is essential for evaluating the performance and generalizability of machine learning models. By using data that the model has not encountered during training, we can assess its ability to handle new scenarios. This section highlights the strengths and limitations of our models in real-world applications, offering insights into potential improvements and optimizations using FMCW sensors. For human detection, we employed a Random Forest (RF) model trained with the top 10 features (time domain and frequency domain features), achieving 95% accuracy on the test data. For action recognition, we utilized a KNN (k=7) model trained on 20 features, which achieved 79% accuracy for three-class action recognition. Due to challenges with the three-class classification, slow and fast movement classes have been merged into a single "movement" class, resulting in a binary classification with static and movement classes. The RF model reached 89% accuracy for this classification. The out-of-sample test

results across various scenarios are presented to thoroughly assess the models under different conditions, providing a comprehensive understanding of their capabilities and limitations in real-world applications. Figure 5.10 shows the scenarios that tested.

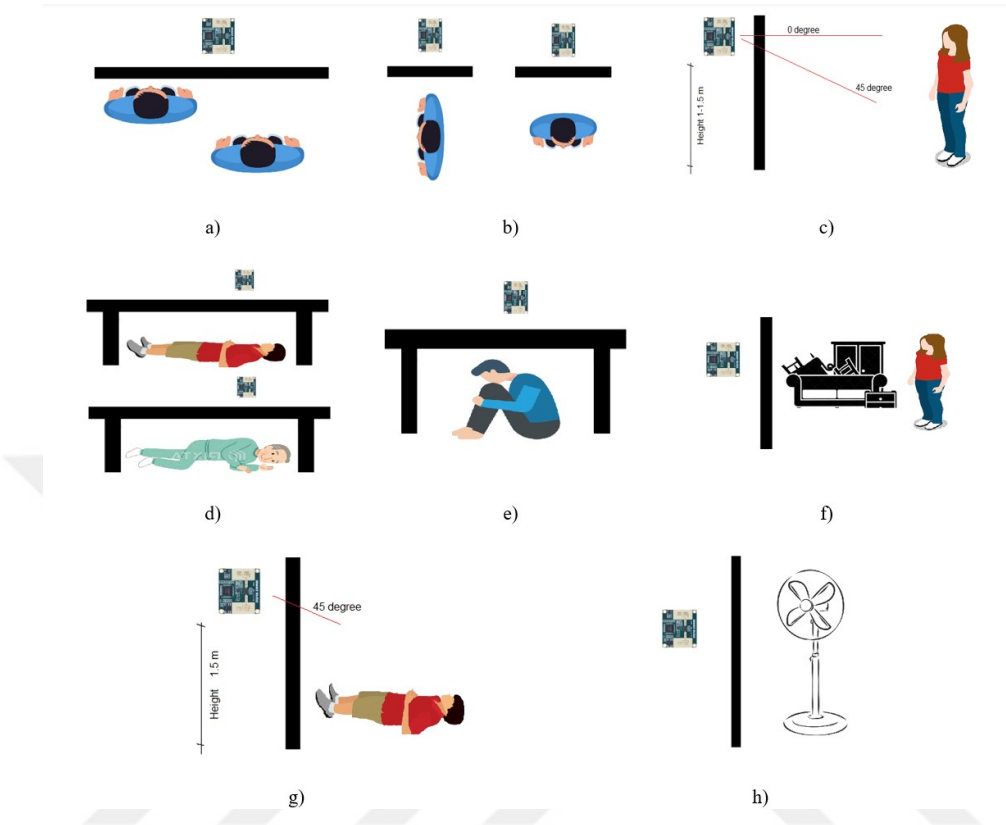



**Figure 5.10** Out-of-test samples a) Multiple People. b) Different Position; 90 Degree and Back Side. c) Change Height and Angle of the Sensor, 1.5m 45 Degree. d) Laying Under Table. e) Siting Under Table. f) Furniture Obstacles Between Wall and Human. g) Laying Behind Wall. h) Non-Human Motion.

The performance of the human detection and action recognition model varies significantly across different scenarios, as indicated by the results in the tables below.

- For binary classification, models achieve a high accuracy to detect humans in different scenarios. However, it still struggles with non-human movements like a fan, which are often misclassified as human presence.
- For action recognition below is detailed explanation.

In table 5.6, the scenario involving multiple people behind a wall, the model shows varied performance. When two individuals are static, the model often misclassifies this as slow movement due to the presence of multiple static signals. In mixed scenarios, where one person is static and the other is moving slowly, the model primarily detects the moving individual, indicating its tendency to focus on movement. When two individuals are moving slowly, the detection accuracy improves, though some misclassification still occurs. Moreover, when four individuals behind wall it also misclassified it as movement due many people breathing movement.

**Table 5.6** Multiple People Behind Wall

| Scenario | Description | Samples | Model prediction (human/ no human) | Action recognition metrics | Observation |
|---|---|---|---|---|---|
| **Two People Static** | Both individuals are static behind the wall. | 22 | Human | TP=7, TN=15<br>Precision=100<br>Recall=32<br>F1-score=48<br>Accuracy=32 | Classifies as movement for most of the samples due to multiple static signals. |
| **One Static, One Moving Slowly** | One person is static, the other is moving slowly | 22 | Human | TP=6, TN=16<br>Precision=100<br>Recall=73<br>F1-score=84<br>Accuracy=73 | Primarily detects the moving individual in mixed scenarios. |
| **Both Moving Slowly** | Both individuals are moving slowly. | 16 | Human | TP=6, TN=10<br>Precision=100<br>Recall=62<br>F1-score=77<br>Accuracy=62 | Detection is fairly accurate but still some misclassification. |
| **Four People Static** | Four individuals are static behind the wall. | 50 | Human | TP=11, TN=39<br>Precision=100<br>Recall=22<br>F1-score=36<br>Accuracy=22 | Classifies as movement for most of the samples due to multiple static signals. |

In table 5.7, For individuals standing static at 90 degrees, the model performs reasonably well, though some confusion with slow movement is observed. However, when individuals are standing static with their back to the sensor (180 degrees), the model struggles significantly, with many instances misclassified as slow or fast movement. This suggests that the model finds it more challenging to detect human presence and classify actions correctly when the individuals are not directly facing the sensor. Moreover, changing the sensor height and angle to 1.5 meters at 45 degrees impacts the model's performance in various ways.

- For static individuals, the model's performance remains similar to that at normal height, with some misclassifications.
- When individuals are moving slowly or fast, the model generally performs well but still shows instances of misclassification, particularly confusing slow movements with static or fast actions.
- For individuals standing static at 90 degrees, performance remains consistent with previous observations. However, for individuals standing static at 180 degrees, significant misclassifications occur, primarily as slow movement.
- For individuals laying behind a wall, the model struggles significantly with static signals. Many static instances are misclassified as slow movements. This indicates that the model has difficulty accurately recognizing human presence and actions when individuals are in a laying position, further highlighting the challenges in different postures.

**Table 5.7** Change Person Standing Angle and Sensor Installation Setup

| Scenario | Description | Samples | Model prediction (human/ no human) | Action recognition metrics | Action Recognition Observation |
|---|---|---|---|---|---|
| **90 degree static** | Human behind wall standing static at 90 degrees relative to sensor. | 50 | Human | TP=14, TN=36<br>Precision=100<br>Recall=28<br>F1-score=44<br>Accuracy=28 | Some confusion with movement. |
| **180 degree (back side) static** | Human behind wall standing static at 180 degrees relative to sensor. | 50 | Human | TP=9, TN=41<br>Precision=100<br>Recall=18<br>F1-score=31<br>Accuracy=18 | Struggles more with back-facing individuals; many classified as slow or fast movement. |
| **Laying** | Individual static behind wall. | 50 | Human | TP=4, TN=46<br>Precision=100<br>Recall=8<br>F1-score=15<br>Accuracy=8 | Struggles with static signals in laying position; many misclassified as slow movement. |
| **Changing sensor height and angle 1.5 m 45 degree** | | | | | |
| **Static** | Individual static behind wall. | 50 | Human | TP=18, TN=32<br>Precision=100<br>Recall=36<br>F1-score=53<br>Accuracy=36 | Performance similar to normal height; some classification but generally accurate. |
| **Slow** | Individual moving slow behind wall. | 50 | Human | TP=18, TN=32<br>Precision=100<br>Recall=64<br>F1-score=78<br>Accuracy=64 | Generally accurate but some instances classified as static. |
| **Fast** | Individual moving fast behind wall. | 50 | Human | TP=16, TN=34<br>Precision=100<br>Recall=68<br>F1-score=81<br>Accuracy=68 | Fair accuracy but some instances classified as static. |
| **90 degree static** | Human behind wall standing static at 90 degrees relative to sensor. | 50 | Human | TP=15, TN=35<br>Precision=100<br>Recall=30<br>F1-score=46<br>Accuracy=30 | Similar performance to previous 90-degree scenario. |
| **180 degree (back side) static** | Human behind wall standing static at 180 degrees relative to sensor. | 50 | Human | TP=4, TN=46<br>Precision=100<br>Recall=8<br>F1-score=15<br>Accuracy=8 | Many instances detected as slow movement. |

Table 5.8, introducing furniture between the sensor and the individuals at a height of 1.5 meters and 45 degrees angle further affects the model's accuracy. For static individuals, the performance drops slightly, leading to more misclassifications. When individuals are moving slowly, the model faces similar issues, struggling to distinguish between static and slow movements. For fast-moving individuals, performance improves, though some instances are still misclassified as slow.

In table 5.9, individuals are positioned under a table, the model's performance declines significantly.

**Table 5.8** Obstacles Between Wall And Human

| Scenario | Description | Samples | Model prediction (human/ no human) | Action recognition metrics | Action Recognition Observation |
|---|---|---|---|---|---|
| **Static** | Individual static behind wall. | 50 | Human | TP=6, TN=44<br>Precision=100<br>Recall=12<br>F1-score=21<br>Accuracy=12 | Performance drops slightly due to furniture. |
| **Slow** | Individual moving slow behind wall. | 50 | Human | TP=12, TN=38<br>Precision=100<br>Recall=76<br>F1-score=86<br>Accuracy=76 | Similar issues as with static; difficulty in distinguishing between static and slow movements. |
| **Fast** | Individual moving fast behind wall. | 50 | Human | TP=12, TN=38<br>Precision=100<br>Recall=76<br>F1-score=86<br>Accuracy=76 | Better performance but some classification as static. |

For static individuals viewed from the side, there is a substantial number of misclassifications. At 90 degrees, the misclassification rate remains high, with many instances detected as slow or fast movements. For sitting individuals which is similar to earthquake "drop, cover, hold", the model often misclassifies them as slow or fast, indicating poor performance in these scenarios. When individuals are waving, the model's performance is mixed, with some waving motions detected as slow but many misclassified.

**Table 5.9** Under Table Scenarios

| Scenario | Description | Samples | Model prediction (human/ no human) | Action recognition metrics | Action Recognition Observation |
|---|---|---|---|---|---|
| **Static** | Individual static under table side view. | 50 | Human | TP=10, TN=40<br>Precision=100<br>Recall=20<br>F1-score=33<br>Accuracy=20 | Performance drops; significant number of static movements classified as movement. |
| **90 degree static** | Individual static under table 90 degree. | 50 | Human | TP=3, TN=47<br>Precision=100<br>Recall=6<br>F1-score=11<br>Accuracy=6 | Many instances detected as slow or fast. |
| **Sitting** | Individual sitting behind wall. | 50 | Human | - | All sitting individuals detected as movement. |
| **Waving** | Individual waving behind wall. | 50 | Human | TP=12, TN=38<br>Precision=100<br>Recall=76<br>F1-score=86<br>Accuracy=76 | Some waving motions detected as static. |

In table 5.10, the presence of non-human movements, such as a fan operating behind a wall, poses a significant challenge for the model. It frequently misclassifies these non-human signals as human

presence, often detecting them as slow movements. This highlights a critical area for improvement, where the model needs to better differentiate between human and non-human signals to avoid false positives.

**Table 5.10** Non-Human Movement

| **Scenario** | **Description** | **Samples** | **Model prediction (human/ no human)** | **Action recognition metrics** | **Action Recognition Observation** |
|---|---|---|---|---|---|
| **Fan** | A fan is operating behind the wall. | 50 | Misclassification as human | TP=6, TN=44<br>Precision=100<br>Recall=88<br>F1-score=94<br>Accuracy=88 | Misclassified as human with movement. |

We can Observe that:

- Binary Classification: The binary classification model is generally effective in distinguishing human from non-human presence but struggles with non-human movements like fans.
- Action Recognition: The action recognition model performs reasonably well for moving individuals but often misclassifies static movements, particularly in complex scenarios.
- Sensor Angle and Height: Changing the sensor angle and height affects the model's accuracy, especially for distinguishing between static and slow movements.
- Obstacles: The presence of obstacles, like furniture, further reduces the model's accuracy, leading to more misclassifications.
- Environmental Challenges: Different positions, such as under a table or laying down, and non-human movements, like a fan, present significant challenges, indicating areas for improvement in model robustness and accuracy

# 6
# CONCLUSION

This thesis investigates the comparative performance of various machine learning algorithms for human detection and activity recognition through walls using a 24 GHz Frequency Modulated Continuous Wave (FMCW) radar sensor. Multiple sensors, including 3.2 GHz CW, 10 GHz CW, and 24 GHz FMCW radar sensors, were explored for their efficacy in detecting human presence behind walls, with the 24 GHz FMCW radar sensor selected for its good performance. Data for this study includes various scenarios involving multiple individuals and a range of activities behind different types of walls. The dataset consists of a total of 556 instances, with 208 samples classified as Class 0 (indicating no human presence), and 348 samples classified as Class 1 (indicating human presence, including 125 static, 98 fast movement, and 125 slow movement). The data was collected and preprocessed to ensure consistency and quality. The study highlights the crucial role of feature selection in enhancing the performance of machine learning models for human detection and activity recognition. A total of 27 features were extracted from the data, encompassing statistical, time domain, and frequency domain characteristics. Feature selection was then conducted through a detailed ranking process using three different feature importance methods: Random Forest, Recursive Feature Elimination (RFE), and Information Gain. The scores and ranks from each method were combined to determine a median and final rank for each feature. These ranked features were then used in varying set sizes (5, 10, 15, 20, and all features) to train human detection models. Six prominent algorithms were evaluated: Support Vector Machine (SVM), K-Nearest Neighbors (KNN), Decision Tree (DT), Naive Bayes (NB), Logistic Regression (LR), and Random Forest (RF). Simpler models with fewer features proved more effective for binary classification tasks. For instance, the Random Forest algorithm achieved an accuracy of 95% with a 10-feature set, demonstrating that a streamlined feature set can capture essential patterns for accurately detecting human presence. This finding suggests that in applications where distinguishing between human presence and absence is critical, a reduced, well-selected feature set can significantly enhance model performance while minimizing computational complexity. Conversely, for multi-class classification tasks, which involve distinguishing between different human activities through a wall, a comprehensive feature set proved more beneficial. The KNN (k=7) algorithm achieved an accuracy of 79% with 10 features, followed closely by Random Forest with 77% accuracy using 5, 10, and 15 features. Other algorithms, such as Decision Tree, also performed well with larger feature sets, achieving accuracies up to 73% with all features. However, Naive Bayes consistently lagged behind the other models, with accuracies ranging from 54% to 61%, highlighting its limitations in handling complex, high-dimensional data. Due to the challenges faced with the three-class classification, the slow and fast movement classes were merged

into a single "movement" class, resulting in a binary classification problem with the classes being static and movement. The RF model achieved 90% accuracy with binary action classification. Moreover, out-of-sample tests confirmed these results, showing the RF model consistently performed well in real-world scenarios involving multiple individuals and mixed activities. Out-of-sample testing validated these findings, demonstrating the robustness and generalizability of the RF model across diverse real-world scenarios. Notably, in scenarios involving two static individuals, the model often misclassified them as slow movement. However, it accurately classified slow movements when both individuals were moving slowly and predominantly detected the moving individual in mixed scenarios. These findings suggest the need for further training with multiple-person data to enhance the model's robustness and accuracy in more complex environments. Despite these promising results, several limitations must be acknowledged. The study was conducted using a specific dataset, and the generalizability of the findings to other datasets or environments may be limited. Lastly, the results indicate that while the current setup can effectively detect and classify human activities behind walls up to a certain extent, there are significant limitations due to the sensor's inability to penetrate materials thicker than 20 centimeters. Future research should:

- Test models on diverse datasets (different wall types and thicknesses, different actions) to validate generalizability.
- Investigate the integration of models into real-time systems and real post-disaster environments.
- Explore advanced techniques like deep learning or hybrid models.
- Expand the scope of the study to include more complex activities or interactions for a comprehensive understanding of human activity recognition.
- Use multiple sensors to improve accuracy.

In conclusion, the 24 GHz FMCW radar sensor proved to be a highly effective approach in detecting human presence and activities behind walls, providing a robust foundation for further advancements in this field. The study demonstrates that strategic feature selection is vital for optimizing the performance of machine learning models in human detection and activity recognition through wall applications. By carefully selecting the number and type of features, it is possible to develop models that are not only highly accurate but also generalizable and efficient.

# REFERENCES


[1] S. Xie, D. Ming, J. Yan, H. Yang, R. Liu, and Z. Zhao, “Research on Fine Estimation of People Trapped after Earthquake on Single Building Level Based on Multi-Source Data,” Applied Sciences (Switzerland), vol. 13, no. 9, May 2023, doi: 10.3390/app13095430.

[2] K. Shirke and B. Iyer, “Through the wall human detection & surveillance sensor,” International Journal of System Assurance Engineering and Management, vol. 14, pp. 569–574, Mar. 2023, doi: 10.1007/s13198-022-01853-5.

[3] A. Soumya, C. Krishna Mohan, and L. R. Cenkeramaddi, “Recent Advances in mmWave-Radar-Based Sensing, Its Applications, and Machine Learning Techniques: A Review,” Sensors (Basel, Switzerland), vol. 23, no. 21. Nov. 01, 2023. doi: 10.3390/s23218901.

[4] Seeed Studio, "24GHz mmWave Sensor - Human Static Presence Module (MR24HPB1)," Seeed Wiki. [Online]. Available: `https://wiki.seeedstudio.com/Radar_MR24HPB1/`. [Accessed: June, 2024].

[5] X. Li, Y. He, and X. Jing, “A survey of Deep Learning-based human activity recognition in Radar,” Remote Sensing, vol. 11, no. 9, p. 1068, 2019. doi:10.3390/rs11091068 5

[6] S. Ahmed et al., “Human Detection Techniques for Search and Rescue of Trapped Victims Under Debris: A Review,” Evolution of Information, Communication and Computing Systems (EICCS), 2022.6

[7] D. Zhang et al., “Evaluation of a sensor system for detecting humans trapped under rubble: A pilot study,” Sensors, vol. 18, no. 3, p. 852, 2018. doi:10.3390/s18030852 7

[8] N. T. P. Van, L. Tang, V. Demir, S. F. Hasan, N. D. Minh, and S. Mukhopadhyay, “Review-microwave radar sensing systems for search and rescue purposes,” Sensors (Switzerland), vol. 19, no. 13, Jul. 2019, doi: 10.3390/s19132879.

[9] S. K. Pramanik and S. M. M. Islam, “Through the wall human heart beat detection using single channel CW radar,” Front Physiol, vol. 15, 2024, doi: 10.3389/fphys.2024.1344221.

[10] G. Gennarelli, G. Ludeno, and F. Soldovieri, “Real-time through-wall situation awareness using a microwave doppler radar sensor,” Remote Sens (Basel), vol. 8, no. 8, 2016, doi: 10.3390/rs8080621.

[11] M. Ritchie, M. Ash, Q. Chen, and K. Chetty, “Through wall radar classification of human micro-doppler using singular value decomposition analysis,” Sensors (Switzerland), vol. 16, no. 9, Sep. 2016, doi: 10.3390/s16091401.

[12] H. Lee, B. H. Kim, J. K. Park, and J. G. Yook, “A novel vital-sign sensing algorithm for multiple subjects based on 24-GHz FMCW Doppler radar,” Remote Sens (Basel), vol. 11, no. 10, May 2019, doi: 10.3390/rs11101237.

[13] F. Qi, F. Liang, H. Lv, C. Li, F. Chen, and J. Wang, "Detection and classification of finer-grained human activities based on stepped-frequency continuous-wave through-wall radar," Sensors (Switzerland), vol. 16, no. 6, Jun. 2016, doi: 10.3390/s16060885.

[14] C. Shi, Z. Zheng, J. Pan, Z. K. Ni, S. Ye, and G. Fang, "Multiple Stationary Human Targets Detection in Through-Wall UWB Radar Based on Convolutional Neural Network," Applied Sciences (Switzerland), vol. 12, no. 9, May 2022, doi: 10.3390/app12094720. 14

[15] K. Sharma, R. Doriya, S. K. Pandey, A. Kumar, G. R. Sinha, and P. Dadheech, "Real-Time Survivor Detection System in SaR Missions Using Robots," Drones, vol. 6, no. 8, Aug. 2022, doi: 10.3390/drones6080219. 15

[16] S. Solaiman, E. Alsuwat, and R. Alharthi, "Simultaneous Tracking and Recognizing Drone Targets with Millimeter-Wave Radar and Convolutional Neural Network," Applied System Innovation, vol. 6, no. 4, Aug. 2023, doi: 10.3390/asi6040068. 16

[17] S. Bjorklund and N. Wadstromer, "Target Detection and Classification of Small Drones by Deep Learning on Radar Micro-Doppler," in 2019 International Radar Conference, RADAR 2019, Institute of Electrical and Electronics Engineers Inc., Sep. 2019. doi: 10.1109/RADAR41533.2019.171294. 17

[18] M. Paul, M. E. Haque, and S. Chakraborty, "Human detection in surveillance videos and its applications-a review," 2013. [Online]. Available: http://asp.eurasipjournals.com/content/2013/1/176 18

[19] C. Shi et al., "Multiple stationary human targets detection in through-wall UWB radar based on convolutional neural network," Applied Sciences, vol. 12, no. 9, p. 4720, 2022. doi:10.3390/app12094720

[20] Y. Jia et al., "ResNet-based counting algorithm for moving targets in through-the-wall radar," IEEE Geoscience and Remote Sensing Letters, vol. 18, no. 6, pp. 1034–1038, 2021. doi:10.1109/lgrs.2020.2990742

[21] Q. An et al., "RPCA-based high resolution through-the-wall human motion feature extraction and classification," IEEE Sensors Journal, vol. 21, no. 17, pp. 19058–19068, 2021. doi:10.1109/jsen.2021.3088122

[22] X. Liang, J. Deng, H. Zhang, and T. A. Gulliver, "Ultra-wideband impulse radar through-wall detection of vital signs," Scientific Reports, vol. 8, no. 1, 2018. doi:10.1038/s41598-018-31669-y

[23] J. Zhang et al., "A multi-target localization and vital sign detection method using ultra-wide band Radar," Sensors, vol. 23, no. 13, p. 5779, 2023. doi:10.3390/s23135779

[24] S. Wang, Q. An, S. Li, G. Zhao, and H. Sun, "Wiring effects mitigation for through-wall human motion micro-doppler signatures using a generative adversarial network," IEEE Sensors Journal, vol. 21, no. 8, pp. 10007–10016, 2021. doi:10.1109/jsen.2021.3057592

[25] X. Liang, Y. Wang, S. Wu, and T. Gulliver, "Experimental study of wireless monitoring of human respiratory movements using UWB impulse radar systems," Sensors, vol. 18, no. 9, p. 3065, 2018. doi:10.3390/s18093065

[26] T. Saeed et al., "Human motion detection through wall based on micro-doppler using Kalman filter combined with convolutional neural network," International Journal of Intelligent Engineering and Systems, vol. 12, no. 4, pp. 317–327, 2019. doi:10.22266/ijies2019.0831.29

[27] D. Uzunidis, E. Margaritis, C. Chatzigeorgiou, C. Z. Patrikakis, and S. A. Mitilineos, "A dataset for aftermath victim detection behind walls or obstacles using an UWB radar sensor," 2023 12th International Conference on Modern Circuits and Systems Technologies (MOCAST), 2023. doi:10.1109/mocast57943.2023.10176448

[28] Harikesh, S. S. Chauhan, A. Basu, M. P. Abegaonkar, and S. K. Koul, "Through the Wall Human Subject Localization and Respiration Rate Detection Using Multichannel Doppler Radar," IEEE Sensors Journal, vol. 21, no. 2, pp. 1510–1518, Jan. 2021, doi: https://doi.org/10.1109/jsen.2020.3016755.

[29] A. Kılıç, İ. Babaoğlu, A. Babalık, and A. Arslan, "Through-wall radar classification of human posture using convolutional neural networks," International Journal of Antennas and Propagation, vol. 2019, pp. 1–10, 2019. doi:10.1155/2019/7541814

[30] D. Shi et al., "A novel non-contact detection and identification method for the post-disaster compression state of injured individuals using UWB Bio-Radar," Bioengineering, vol. 10, no. 8, p. 905, 2023. doi:10.3390/bioengineering10080905

[31] P. Chen et al., "Through-wall human motion recognition based on Transfer Learning and ensemble learning," IEEE Geoscience and Remote Sensing Letters, vol. 19, pp. 1–5, 2022. doi:10.1109/lgrs.2021.3070374

[32] L. Pham, M. Paul, and C. Withana, "Detecting trapped humans through chest wall movements with non-contact Doppler sensor," 2019 IEEE 9th Symposium on Computer Applications & Industrial Electronics (ISCAIE), 2019. doi:10.1109/iscaie.2019.8743708

[33] X. Xu, S. Zeng, and J. Liu, "Human body micro-doppler signal detection technology based on CW Doppler radar," 2022 IEEE 4th International Conference on Power, Intelligent Computing and Systems (ICPICS), 2022. doi:10.1109/icpics55264.2022.9873706

[34] L. Pham, M. Paul, and P. Prasad, "Noncontact detection of cardiopulmonary activities of trapped humans in rescue relief events," IEEE Access, vol. 10, pp. 75680–75692, 2022. doi:10.1109/access.2022.3190902

[35] Z. Duan and J. Liang, "Non-contact detection of vital signs using a UWB radar sensor," IEEE Access, vol. 7, pp. 36888–36895, 2019. doi:10.1109/access.2018.2886825

[36] A. A. Pramudita et al., "Radar system for detecting respiration vital sign of live victim behind the wall," IEEE Sensors Journal, vol. 22, no. 15, pp. 14670–14685, 2022. doi:10.1109/jsen.2022.3188165

[37] Z. Li, T. Jin, Y. Dai, and Y. Song, "Through-wall multi-subject localization and vital signs monitoring using UWB MIMO Imaging radar," Remote Sensing, vol. 13, no. 15, p. 2905, 2021. doi:10.3390/rs13152905

[38] J. Pan et al., "A multi-target detection method based on improved U-Net for UWB MIMO through-wall radar," Remote Sensing, vol. 15, no. 13, p. 3434, 2023. doi:10.3390/rs15133434

[39] B. P. Rohman, M. Andra, and M. Nishimoto, "Through-the-wall human respiration detection using UWB impulse radar on hovering drone," IEEE Journal of Selected Topics in Applied Earth Observations and Remote Sensing, vol. 14, pp. 6572–6584, 2021. doi:10.1109/jstars.2021.3087668

[40] A. Sarkar and D. Ghosh, "Through-wall heartbeat frequency detection using Ultra-Wideband Impulse Radar," 2019 International Conference on Range Technology (ICORT), 2019. doi:10.1109/icort46471.2019.9069632

[41] H. Xu et al., “Through-wall human motion recognition using Random Code radar sensor with multi-domain feature fusion,” IEEE Sensors Journal, vol. 22, no. 15, pp. 15123–15132, 2022. doi:10.1109/jsen.2022.3183292

[42] R. Khanna, D. Oh, and Y. Kim, “Through-wall remote human voice recognition using Doppler radar with transfer learning,” IEEE Sensors Journal, vol. 19, no. 12, pp. 4571–4576, 2019. doi:10.1109/jsen.2019.2901271

[43] V. Singh, S. Bhattacharyya, and P. K. Jain, “Through the wall human signature detection using principle component analysis (PCA),” 2018 IEEE International Symposium on Antennas and Propagation & USNC/URSI National Radio Science Meeting, 2018. doi:10.1109/apusncursinrsm.2018.8609027

[44] F. Ghorbani and H. Soleimani, “Through-the-wall radar under Electromagnetic Complex Wall: A deep learning approach,” Results in Applied Mathematics, vol. 17, p. 100354, 2023. doi:10.1016/j.rinam.2022.100354

[45] Y. Zhang et al., “A coarse-to-fine detection and localization method for multiple human subjects under through-wall condition using a new telescopic Simo UWB radar,” Sensors and Actuators A: Physical, vol. 332, p. 113064, 2021. doi:10.1016/j.sna.2021.113064

[46] S. Maiti and A. Bhattacharya, “Microwave detection of respiration rate of a living human hidden behind an inhomogeneous optically opaque medium,” IEEE Sensors Journal, vol. 21, no. 5, pp. 6133–6144, 2021. doi:10.1109/jsen.2020.3043846

[47] Y. Jia et al., “Detection and localization for multiple stationary human targets based on cross-correlation of dual-station SFCW radars,” Remote Sensing, vol. 11, no. 12, p. 1428, 2019. doi:10.3390/rs11121428

[48] S. Wu, H. Zhou, S. Liu, and R. Duan, “Improved through-wall radar imaging using modified Green’s function-based multi-path exploitation method,” EURASIP Journal on Advances in Signal Processing, vol. 2020, no. 1, 2020. doi:10.1186/s13634-020-0660-2

[49] G. Moro, F. Di Luca, D. Dardari, and G. Frisoni, “Human being detection from UWB NLOS signals: Accuracy and generality of Advanced Machine Learning Models,” Sensors, vol. 22, no. 4, p. 1656, 2022. doi:10.3390/s22041656

[50] F.-K. Wang et al., “See-through-wall (STW) life detector using self-injection-locked (SIL) technology,” 2020 IEEE Asia-Pacific Microwave Conference (APMC), 2020. doi:10.1109/apmc47863.2020.9331560

[51] D. Uzunidis et al., “Real-time human detection behind obstacles based on a low-cost UWB radar sensor,” 2022 IEEE 8th World Forum on Internet of Things (WF-IoT), 2022. doi:10.1109/wf-iot54382.2022.10152170

[52] K. Phaisiri, A. Boonpoonja, C. Kittiyanpunya, K. Kaemarungsi, and N. Chudpooti, “Through-Wall Human Sensing Using mmWave FMCW Radar,” in 4th Research, Invention, and Innovation Congress: Innovative Electricals and Electronics: Innovation for Better Life, RI2C 2023, Institute of Electrical and Electronics Engineers Inc., 2023, pp. 1–4. doi: 10.1109/RI2C60382.2023.10355972.

[53] A. A. Pramudita et al., “Radar System for Detecting Respiration Vital Sign of Live Victim Behind the Wall,” IEEE Sens J, vol. 22, no. 15, pp. 14670–14685, Aug. 2022, doi: 10.1109/JSEN.2022.3188165.

[54] Q. H. Ramadhamy, A. A. Pramudita, and F. Y. Suratman, "Clutter Reduction in Detecting Trapped Human Respiration under Rubble for FMCW Radar System," in 2023 International Seminar on Intelligent Technology and Its Applications: Leveraging Intelligent Systems to Achieve Sustainable Development Goals, ISITIA 2023 - Proceeding, Institute of Electrical and Electronics Engineers Inc., 2023, pp. 716–721. doi: 10.1109/ISITIA59021.2023.10221122.

[55] D. Uzunidis, S. A. Mitilineos, C. Ponti, G. Schettini, and C. Z. Patrikakis, "Detection of trapped victims behind large obstacles using radar sensors: a review on available technologies and candidate solutions," in IEEE Conference on Antenna Measurements and Applications, CAMA, Institute of Electrical and Electronics Engineers, 2023, pp. 1025–1030. doi: 10.1109/CAMA57522.2023.10352910.

[56] W. Wang, D. Wang, B. Zhang, T. Li, and S. Jiang, "Through-Wall Multistatus Target Identification in Smart and Autonomous Systems with UWB Radar," IEEE Internet Things J, vol. 5, no. 5, pp. 3278–3288, Oct. 2018, doi: 10.1109/JIOT.2017.2695644.

[57] G. Moro, F. Di Luca, D. Dardari, and G. Frisoni, "Human Being Detection from UWB NLOS Signals: Accuracy and Generality of Advanced Machine Learning Models," Sensors, vol. 22, no. 4, Feb. 2022, doi: 10.3390/s22041656.

[58] Y. Li, W. Wang, and Y. Jiang, "Through wall human detection under small samples based on deep learning algorithm," IEEE Access, vol. 6, pp. 65837–65844, 2018, doi: 10.1109/ACCESS.2018.2877730.

[59] W. Wang et al., "Human Detection in Realistic Through-the-Wall Environments using Raw Radar ADC Data and Parametric Neural Networks," Mar. 2024, [Online]. Available: http://arxiv.org/abs/2403.15468

[60] A. Wood, R. Wood, and M. Charnley, "Through-the-wall radar detection using machine learning," Results in Applied Mathematics, vol. 7, Aug. 2020, doi: 10.1016/j.rinam.2020.100106.

[61] A. Kılıç, İ. Babaoğlu, A. Babalık, and A. Arslan, "Through-wall radar classification of human posture using convolutional neural networks," Int J Antennas Propag, vol. 2019, 2019, doi: 10.1155/2019/7541814.

[62] D. Uzunidis, P. Kasnesis, E. Margaritis, M. Feidakis, C. Z. Patrikakis, and S. A. Mitilineos, "Real-Time Human Detection Behind Obstacles Based on a low-cost UWB Radar Sensor," in 2022 IEEE 8th World Forum on Internet of Things, WF-IoT 2022, Institute of Electrical and Electronics Engineers Inc., 2022. doi: 10.1109/WF-IoT54382.2022.10152170.

[63] E. Antolinos, F. García-Rial, C. Hernández, D. Montesano, J. I. Godino-Llorente, and J. Grajal, "Cardiopulmonary activity monitoring using millimeterwave radars," Remote Sens (Basel), vol. 12, no. 14, Jul. 2020, doi: 10.3390/rs12142265.

[64] K. E. Park, J. P. Lee, and Y. Kim, "Deep learning-based indoor distance estimation scheme using FMCW radar," Information (Switzerland), vol. 12, no. 2, pp. 1–14, Feb. 2021, doi: 10.3390/info12020080.

[65] L. Cao, S. Liang, Z. Zhao, D. Wang, C. Fu, and K. Du, "Human Activity Recognition Method Based on FMCW Radar Sensor with Multi-Domain Feature Attention Fusion Network," Sensors, vol. 23, no. 11, Jun. 2023, doi: 10.3390/s23115100.

[66] S. W. Kang, M. H. Jang, and S. Lee, "Identification of human motion using radar sensor in an indoor environment," Sensors, vol. 21, no. 7, Apr. 2021, doi: 10.3390/s21072305.

[67] K. Chetty, Q. Chen, M. Ritchie, and K. Woodbridge, “A low-cost through-the-wall FMCW radar for stand-off operation and activity detection,” in Radar Sensor Technology XXI, SPIE, May 2017, p. 1018808. doi: 10.1117/12.2261680.

[68] Y. Wang, W. Wang, M. Zhou, A. Ren, and Z. Tian, “Remote monitoring of human vital signs based on 77-GHZ MM-WAVE FMCW radar,” Sensors (Switzerland), vol. 20, no. 10, May 2020, doi: 10.3390/s20102999.

[69] “24GHz mmWave Sensor Human Static Presence Module Lite User Manual V1.5.” Accessed: July, 2024. [Online]. Available: https://files.seeedstudio.com/wiki/mmWave-radar/MR24HPC1_User_Manual-V1.5.pdf.

[70] “24GHz mmWave Sensor-Human Static Presence Module Lite Datasheet Product Overview Statement,” 2008.Accessed: July, 2024. [Online]. Available: https://files.seeedstudio.com/wiki/mmWave-radar/24GHz_mmWave_Sensor-Human_Static_Presence_Module_Lite_Datasheet.pdf.

[71] Seeed Studio, "24GHz mmWave Sensor - Human Static Presence Module Lite (MR24HPC1)," Accessed: June, 2024. [Online]. Available: https://wiki.seeedstudio.com/Radar_MR24HPC1/.

[72] B. Scholkopf and A. J. Smola, Learning with Kernels: Support Vector Machines, Regularization, Optimization, and Beyond. MIT Press, 2002.

[73] T. M. Cover and P. E. Hart, "Nearest neighbor pattern classification," IEEE Transactions on Information Theory, vol. 13, no. 1, pp. 21-27, Jan. 1967

[74] D. W. Hosmer, S. Lemeshow, and R. X. Sturdivant, Applied Logistic Regression, 3rd ed. Hoboken, NJ, USA: Wiley, 2013.

[75] H. Zhang, "The optimality of naive Bayes," in Proceedings of the Seventeenth International Florida Artificial Intelligence Research Society Conference (FLAIRS 2004), 2004, pp. 562-567.

[76] L. Breiman, J. Friedman, R. A. Olshen, and C. J. Stone, "Classification and Regression Trees", 1st ed. Boca Raton, FL, USA: Chapman and Hall/CRC, 1984. [Online]. Available: https://doi.org/10.1201/9781315139470.

[77] A. Liaw and M. Wiener, "Classification and regression by randomForest," R News, vol. 2, no. 3, pp. 18-22, Dec. 2002.

[78] N9916A FieldFox Handheld Microwave Analyzer, 14 GHz. Accessed: July, 2024. [Online]. Available: https://www.keysight.com/us/en/product/N9916A/fieldfox-a-handheld-microwave-analyzer-14-ghz.html.

[79] YSR-120 Handheld, Through Wall Radar. Accessed: July, 2024. [Online]. Available: https://www.bjltsj.com/en/product/1004.html.

[80] Xaver™ 400 Through wall imaging system. Accessed: July, 2024. [Online]. Available: availableathttps://camero-tech.com/xaver-products/xaver-400/.

# A
# SORTED FEATURES FOR ACTION RECOGNITION

**Table A.1** Sorted Features for Action Recognition

| **Feature** | **Combined Importance** |
|---|---|
| Median | 0.449079 |
| xmin | 0.445877 |
| Mean | 0.441026 |
| Entropy | 0.430600 |
| Form Factor | 0.405570 |
| SD/mean ratio | 0.405448 |
| Variance | 0.383180 |
| SHANNON_Entropy | 0.381395 |
| Max/min ratio | 0.358682 |
| Mobility | 0.355367 |
| Kurtosis | 0.197644 |
| Max - min squared | 0.179665 |
| RMS | 0.158006 |
| Power | 0.123504 |
| Energy | 0.106461 |
| Total_Power | 0.097485 |
| Max - min | 0.091786 |
| Skewness | 0.089538 |
| Std.deviation | 0.087841 |
| FSkewness | 0.084799 |
| Correlation | 0.078189 |
| FVariance | 0.069812 |
| FKurtosis | 0.069164 |
| Mean_Frequency | 0.063366 |
| xMax | 0.046174 |
| median_frequency | 0.045349 |
| Turns Count | 0.029928 |

# PUBLICATIONS FROM THE THESIS

## Conference Papers

1. Z. Malik et al.,"Feature Engineering to Detect People Behind Walls Using UWB Sensor",The 32nd IEEE Conference on Signal Processing and Communications Applications, 2024.